

# Investigation of $[\text{N-X-N}]^+$ and $[\text{N-C-N}]^+$ Complexes in Solution

Exploring Geometry, Stability and Symmetry

Alavi Karim



UNIVERSITY OF GOTHENBURG

Department of Chemistry and Molecular Biology

University of Gothenburg

2017

DOCTORAL THESIS

Submitted for fulfilment of the requirements for the degree of  
Doctor of Philosophy in Chemistry

Investigation of [N-X-N]<sup>+</sup> and [N-C-N]<sup>+</sup> Complexes in Solution  
Exploring Geometry, Stability and Symmetry

© Alavi Karim

ISBN: 978-91-629-0334-3 (Print)

ISBN: 978-91-629-0335-0 (PDF)

<http://hdl.handle.net/2077/52372>

Department of Chemistry and Molecular Biology

SE-41296 Göteborg

Sweden

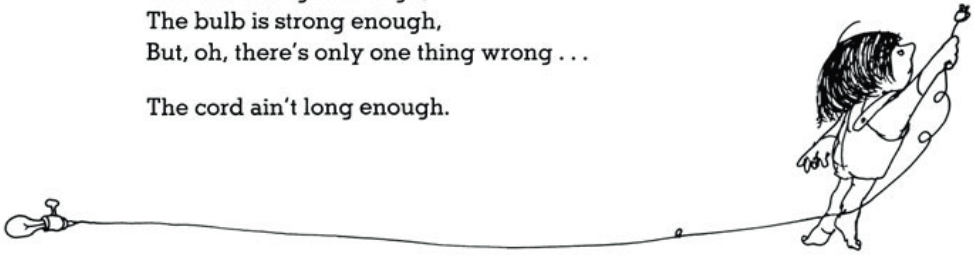
Printed by BrandFactory AB

Källered, 2017

## INVENTION

I've done it, I've done it!  
Guess what I've done!  
Invented a light that plugs into the sun.  
The sun is bright enough,  
The bulb is strong enough,  
But, oh, there's only one thing wrong . . .

The cord ain't long enough.



- Shel. S

To my loving brothers,  
Atif, Yasir and Yazdaan



# Abstract

---

Halogen bonding is a weak interaction. In this thesis the three center four electron halogen bond,  $[\text{N}-\text{X}-\text{N}]^+$ , has been studied. The lighter halogens form highly unstable halonium ions that are reactive towards nucleophiles and their complexes were therefore investigated at low temperatures. Whereas the chlorine-centered halogen bond was found to be symmetric, the fluorine-centered one is shown to be asymmetric in solution. These geometries have been determined by NMR spectroscopic evidences and computations at the DFT level. For determining the influence of the counterion on the iodine-centered halogen bond, the isotopic perturbation of equilibrium (IPE) technique was applied with  $^{13}\text{C}$   $\{^1\text{H}, ^2\text{H}\}$  NMR detection in solution, and X-ray diffraction in the solid state. The symmetric arrangement of  $[\text{N}-\text{I}-\text{N}]^+$  complexes possessing two equal N-I halogen bonds remains undisturbed, independent of the choice of counterion and also when it has been scavenged. In comparison, silver centered  $[\text{N}-\text{Ag}-\text{N}]^+$  complexes although similar in size to the iodonium center, show direct counterion coordination to the metal center.

The three center four electron complex of a positively charged carbenium ion trapped between two nitrogenous donors forming a thermodynamically stable pentavalent  $[\text{N}-\text{C}-\text{N}]^+$  complex has also been studied. The structure and properties of this complex is discussed based on NMR spectroscopic and reaction kinetic evidences in comparison to the analogous three-centered  $[\text{N}-\text{X}-\text{N}]^+$  halogen bond. A geometrically restrained bidentate Lewis base is shown to be necessary for the formation of this pentavalent complex. NMR spectroscopic and X-ray crystallographic evidences indicate that a monodentate Lewis base induces a reaction instead of stabilizing the reactive species as a thermodynamically stable complex. As the geometry of the pentavalent complex greatly resembles the  $\text{S}_{\text{N}}2$  transition state, it affords a smoothly modifiable model system for the investigation of fundamental reaction mechanisms and chemical bonding theories

---

Keywords: three center four electron, halonium, carbenium, carbonium, pentavalent, symmetry, isotopic perturbation of equilibrium, NMR, variable temperature, counterion

# List of publications

---

This thesis is based on the following papers and manuscripts which are referred to in the text by their Roman numerals **I-III**. Reprints were made with permission from the The Royal Society of Chemistry

## **I. The nature of [N–Cl–N]<sup>+</sup> and [N–F–N]<sup>+</sup> halogen bonds in solution**

Alavi Karim, Marcus Reitti, Anna-Carin C. Carlsson, Jürgen Gräfenstein and Máté Erdélyi

*Chem. Sci.*, **2014**, 5, 3226

## **II. Counterion influence on the N–I–N halogen bond**

Michele Bedin,<sup>‡</sup> Alavi Karim,<sup>‡</sup> Marcus Reitti, Anna-Carin C. Carlsson, Filip Topi Mario Cetina, Fangfang Pan, Vaclav Havel, Fatima Al-Ameri, Vladimir Sindelar, Kari Rissanen, Jürgen Gräfenstein and Máté Erdélyi

<sup>‡</sup> Shared first author

*Chem. Sci.*, **2015**, 6, 3746

## **III. Pentavalent Carbonium Ions in Solution**

Alavi Karim, Nils Schulz, Hanna Andersson, Bijan Nekouesihahraki, Sandro Keller, Jürgen Gräfenstein, Máté Erdélyi

*Manuscript.*, **2017**

**Substituent Effects on the [N–I–N]<sup>+</sup> Halogen Bond**

Anna-Carin C. Carlsson, Krenare Mehmeti, Martin Uhrbom, [Alavi Karim](#), Michele Bedin, Rakesh Puttreddy, Roland Kleinmaier, Alexei A. Neverov, Bijan Nekoueishahraki, Jürgen Gräfenstein, Kari Rissanen, and Máté Erdélyi  
*J. Am. Chem. Soc.* **2016**, 138, 9853–9863

**Solvent effects on halogen bond symmetry**

Anna-Carin C. Carlsson, Martin Uhrbom, [Alavi Karim](#), Ulrika Brath, Jürgen Gräfenstein and Máté Erdélyi  
*CrystEngComm*, **2013**, 15, 3087–3092

**Solvent effects on <sup>15</sup>N NMR coordination shifts**

Roland Kleinmaier, Sven Arenz, [Alavi Karim](#), Anna-Carin C. Carlsson and Máté Erdélyi  
*Magn. Reson. Chem.* **2013**, 51, 46–53

**Symmetric Halogen Bonding Is Preferred in Solution**

Anna-Carin C. Carlsson, Jürgen Gräfenstein, Adnan Budnjo, Jesse L. Laurila, Jonas Bergquist, [Alavi Karim](#), Roland Kleinmaier, Ulrika Brath, and Máté Erdélyi  
*J. Am. Chem. Soc.* **2012**, 134, 5706–5715

## Abbreviations

---

XB	Halogen Bonding
HB	Hydrogen Bonding
LB	Lewis base
NMR	Nuclear Magnetic Resonance
HMBC	Heteronuclear Multiple Bond Correlation
DOSY	Diffusion Ordered Spectroscopy
HOESY	Heteronuclear Overhauser Effect Spectroscopy
IPE	Isotopic Perturbation of Equilibrium
VT	Variable Temperature
ZPE	Zero Point Energy
rt	Room temperature
EWG	Electron withdrawing group
NOE	Nuclear Overhauser Effect
DA	Diels Alder
DCM	Dichloromethane
n.d.	Not determined



# Table of Contents

---

<b>1. General Introduction</b> .....	1
<b>2. The Halogen Bond</b> .....	3
2.1. The $\sigma$ hole.....	5
2.2. Halogen vs Hydrogen Bonding.....	7
<b>3. XB applications and examples</b> .....	9
<b>4. Carbocations</b> .....	11
<b>5. Objectives</b> .....	13
<b>6. Paper I</b> .....	15
6.1. Three center four electron.....	15
6.2. Synthesis & NMR of $[\text{NCIN}]^+$ .....	16
6.3. Synthesis & NMR of $[\text{NFN}]^+$ .....	20
6.4. Computation.....	22
6.3. Summary.....	24
<b>7. Paper II</b> .....	25
7.1. Isotopic perturbation of equilibrium (IPE).....	26
7.2. Synthesis, analysis and VT.....	29
7.3. Scavenging the CI.....	33
7.4. XB solid state & <i>in silico</i> .....	35
7.5. Summary.....	36
<b>8. Manuscript III</b> .....	37
8.1. Synthesis.....	38
8.2. NMR.....	39
8.3. DA.....	42
8.4. Summary.....	43
<b>9. Concluding remarks</b> .....	45
<b>10. Acknowledgements</b> .....	47
<b>11. References</b>	



# 1. General Introduction

---

Halogen bonding (XB), an electron density donation based weak interaction between an electrophilic halogen and a Lewis base has gained significant attention due to its versatile applicability in a variety of research fields including crystal engineering,<sup>1</sup> material sciences,<sup>2</sup> medicinal chemistry and organocatalysis.<sup>3,4</sup> To date, over 50% of molecules selected for high throughput screening and one-third of all drugs in therapeutic use contain halogens.<sup>5</sup> It was widely believed that incorporating a halogen into a drug candidate lies in the halogen's ability to increase lipophilicity thereby improving its ability to penetrate through lipid membranes and tissues. However this is not in agreement with a number of observations as for example; the judicious introduction of fluorine into a molecule can productively influence conformation,  $pK_a$ , intrinsic potency and pharmacokinetic properties and not only alter its polarity.<sup>6</sup> This indicates that the halogen is most likely involved in more selective interactions due to their positioning on the periphery of molecules.<sup>7</sup> Therefore a better understanding of their nature could direct design efforts for the incorporation of strategically selected atoms to promote ligand-receptor interaction with more specificity.<sup>7</sup>

Another weak interaction that retains crucial information on some of the most fundamental concepts of organic chemistry are those that are formed and broken during the transition state of a bimolecular nucleophilic substitution reaction. The tetravalency of a carbon atom forming a maximum of four chemical bonds is inherently contradicted by this transition state configuration and therefore properties of stable hypervalent carbon compounds have attracted considerable attention.<sup>8,9,10</sup> During the formation of such high energy intermediates, the central carbon atom adapts a pentavalent configuration with three of its substituents lying in one plane and with the incoming nucleophile and the leaving groups being positioned apically in a linear arrangement.<sup>8</sup> Hence, to achieve a deeper understanding of the labile geometry encompassed by this central carbon during such processes, the *intermolecular* pentavalent complex generated would need to be stabilized to extract critical information.



## 2. The Halogen Bond

---

Although more commonly regarded as electron rich species with high electronegativity, the halogen atom can also function as an electron poor partner in net attractive interactions.<sup>11</sup> The official IUPAC definition of the halogen bond<sup>12</sup> was only released as recently as 2013 and describes the phenomenon to occur when there is an evidence of a net attractive interaction between an electrophilic region associated with the surface of a halogen atom in a molecular entity and a nucleophilic region in another, or the same, molecular entity. This is typically denoted by  $R-X\cdots D$ , where  $R-X$  is the halogen bond donor and  $X$  is any halogen atom (I, Br, Cl and rarely F) that is covalently bound to a group(s)  $R$  and can accept electron density donation from the nucleophilic region of a halogen bond acceptor  $D$  (Figure 1). The nomenclature is, albeit somewhat confusingly, contrary to the conventional definition of a donor-acceptor relationship used for metal complexes, but rather defined in a manner to emphasize similarity to that for hydrogen bonding (HB) whereby the HB donor has the partially positively charged  $[H]^+$  that interacts with a LB. Similarly in XB, although the donor  $D$  donates its electron density to the electrophilic region of the halogen atom, it is defined as the halogen bond acceptor as it accepts the partially positively charged halogen of the halogen bond donor,  $R-X$ . Of the extensive list of features that characterize the halogen bond<sup>12</sup>, those that are most important to the complexes discussed in this thesis are highlighted below:

- It is a non-covalent interaction and the forces that dominate its formation are primarily electrostatic, but polarization, charge transfer and dispersion all play an important role.
- The attractive nature of the X-bond results in the interatomic distance between  $X$  and  $D$  to be less than the sum of the van der Waals radii of the participating atoms. The stronger the interaction, the shorter this distance is.
- The bond formed tends to be close to linear and the angle  $Y-X\cdots D$  close to  $180^\circ$

- The bond strength decreases as electronegativity of the halogen increases rendering fluorine to be the poorest halogen bond donor and iodine the strongest.
- XB effects are usually observable by NMR spectroscopy both in solution and in the solid state.

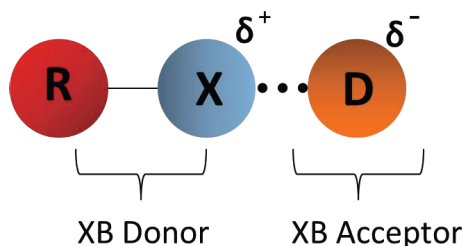


**Figure 1.** Schematic representation of the R—X···D model used to describe XB

Although these interaction types were noticed almost 200 years ago with the formation of an iodine-ammonia complex whereby the iodine accepts electron density donation from the nitrogen of ammonia, it did not receive widespread attention until Odd Hassel received the Nobel Prize in 1969.<sup>13</sup> During the mid-70's Dumas first introduces the term “halogen bonding”, after which the discussion of the interaction type lay dormant for almost a decade as it was thought to occur mostly in the solid state.<sup>14</sup> With the work of Desiraju and Legon, halogen bonding re-emerged in the late 80's and by the late 90's received a considerable amount of interest as Resnati and Metrangolo demonstrated their application in crystal engineering.<sup>15</sup> Over the last decade, halogen bonding has been intensely studied and its existence is now widely accepted.

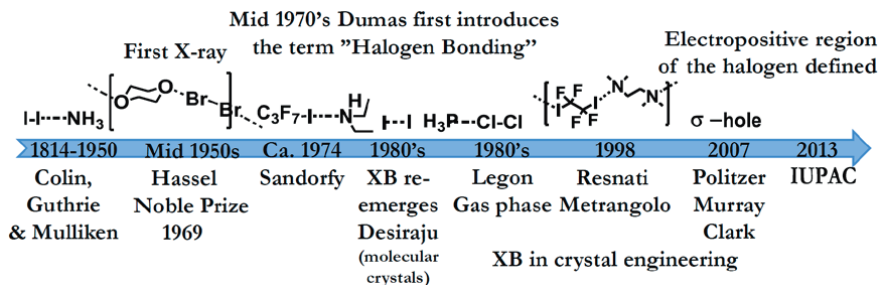
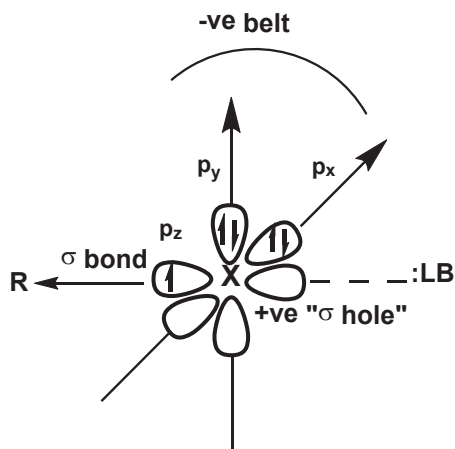


Figure 2. A brief historical timeline of the discovery of XB

## 2.1 The $\sigma$ -hole

In order to understand how electron-rich species such as the halogens can favorably interact with other electronegative sites, Clark et al. have provided an explanation at the molecular orbital level.<sup>16,17</sup> Due to an anisotropic charge distribution that forms when a halogen participates in a covalent interaction, positive electrostatic potential arises on the outermost portion of the surface of the halogen atom which is defined as the “ $\sigma$ -hole” (Figure 3). The term  $\sigma$ -hole arises due to the region of electron density depletion occurring along the extension of the R–X  $\sigma$ -bond in the R–X...D model system; *i.e.* the  $\sigma^*$  orbital of the  $\sigma$  bond. In a covalently bound halogen, where X = F, Cl, Br or I, the halogen follows an approximate  $s^2p_x^2p_y^2p_z^1$  configuration with the RX bond centered along the z-axis. The belt of negative potential develops around the lateral sides of the molecule perpendicular to the R–X bond thereby leaving the outermost portion - opposite the  $\sigma$  bond – with a partial positive charge. This electropositive tip of the halogen can interact favorably with the negative electrostatic potential of an electron donor (Figure 3). The size of the  $\sigma$ -hole, *i.e.*, the extent of the electron density depletion depends on the polarizability and electronegativity of the halogen atom. The more polarizable the halogen is, the more positive is its  $\sigma$ -hole and stronger is the halogen bond that it forms. Therefore the strength of the halogen bond increases in the order of  $I > Br \gg Cl \gg F$  rendering the lighter halogens to be significantly weaker halogen bond donors. The positive character of the  $\sigma$ -hole can also be increased by making the molecular environment around it more electron withdrawing.



**Figure 3.** Electronic configuration followed by a covalently bound halogen ( $p_x^2 p_y^2 p_z^1$ ) that gives rise to the positive electrostatic potential along the z-axis. The charge distribution across the halogen atom's surface becomes anisotropic when it participates in a covalent interaction.

An illustration of the  $\sigma$ -hole concept is shown in Figure 4 using *N*-halopyridinium ions as an example. The size of the  $\sigma$ -hole shown in dark blue consecutively gets smaller as we go from iodine to fluorine (left to right). The positive tip is largest for the most polarizable iodine and almost non-existent for the highly electronegative fluorine. However, it should be emphasized that a purely electrostatic model alone as put forward by the sigma hole description is not sufficient to describe all XB interaction types. Further consideration is therefore required as alternative forces such as charge transfer and dispersion also play key roles.<sup>18,19</sup> All X-bonded systems discussed in this thesis possess significant charge transfer contribution in addition to electrostatics and majority of the systems completely lack  $\sigma$ -holes.



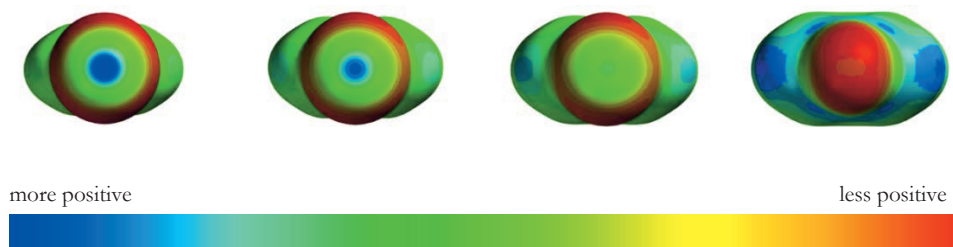


**Figure 4.** The computed surface electrostatic potential of *N*-halopyridinium ions visualizing the  $\sigma$ -hole of I (left), Br, Cl and F(right). The color range denotes most positive to least positive in the order of blue > light blue > green > yellow > red

## 2.2 Halogen vs Hydrogen Bonding

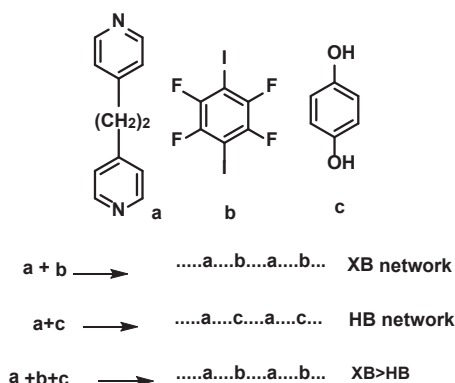
The term halogen bonding - often referred to as the '*long lost brother of the hydrogen bond*' - was introduced to be used analogously with the more widely discussed hydrogen bonding (HB) due to similarities between the two interaction types.<sup>5,20</sup> Although the existence of XB in solution was established earlier,<sup>21</sup> efforts put forward by Desiraju, Resnati and Metrangolo revived the curiosity of the scientific community towards XB.<sup>22-24</sup> Some important donor-acceptor features of the X-Bond ( $R-X\cdots D$ ) and H-Bond ( $R-H\cdots D$ ) are summarized here below.<sup>25-27</sup>

- Both are short range, electrostatically driven, non-covalent interactions between an electropositive halogen or hydrogen (Lewis acidic) and can accept electron density from a donor (Lewis base).
- XB interactions are specific and strongly directional with the  $R-X\cdots D$  angle close to  $180^\circ$  whereas HB directionality falls in between the non-directional van der Waals interaction and the highly directional covalent bond
- The energy of a hydrogen bond lies in the range of 4 to 160  $\text{kJ mol}^{-1}$  and for X-bonds in the range from 5-180  $\text{kJ mol}^{-1}$  with  $I_3^-$  and  $FHF$  being extreme examples.
- Since XBs and HBs share similar sets of acceptors, the two interaction types can compete against each other.



### 3. XB Applications and Examples

Resnati and Metrangolo et al.<sup>28-30</sup> examined the relevance and strength of these non-covalent interactions by using perfluorohydrocarbons as XB donors. As shown by the example in Scheme 1, they highlight the use of halogen bonding in the self-assembly of molecules **a**, **b** and **c** where the recognition pattern controlling the self-assembly process can be either XB or HB. In this scenario, XB not only dominates over HB but also singles out the molecules involved in the construction of supramolecular architectures. Addition of equimolar ratios of **a** and **b** afforded linear chains held together by XB interactions and **a** with **c** generated a hydrogen bonded 1D network. In order to test the competitive ability of XB with that of HB, the three (**a+b+c**) were mixed together and crystals obtained. A remarkable preference was demonstrated for the XB network which crystallizes out whilst **c** remains in the liquid phase.



**Scheme 1.** Schematic representation of XB and HB competition <sup>28</sup>

Rissanen et al. reported the synthesis of dimeric and hexameric capsules solely based on  $[\text{NIN}]^+$  halogen bonds.<sup>31-33</sup> A variety of *N*-donor tripodal ligands participating in the formation of discrete cationic supramolecular halonium cages were presented with either three or six  $[\text{N-I-N}]^+$  connectors securing the two sides

of the cage together (Figure 5). Very similar to the methods discussed in this thesis, they too generate their strongly polarized electrophilic XB donor for forming the linkages by starting with the Ag(I) complex which undergoes a cation exchange process upon reaction with molecular iodine. The halonium ion generated is consequently trapped between the two nitrogenous donors from either side highlighting the strength of these species when constructing such supramolecular assemblies.

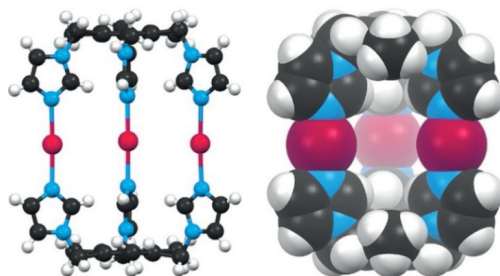
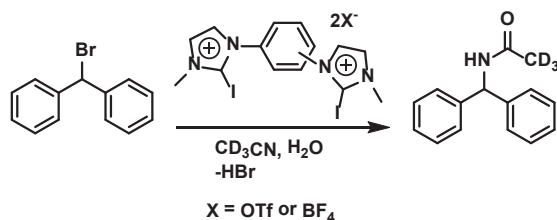


**Figure 5.** Supramolecular cages built based on  $[\text{NIN}]^+$  halogen bonds. <sup>31</sup>

Counterion effects on XB has been demonstrated by the work of Huber et al. (Scheme 2) whereby better conversion of benzhydryl bromide to an amide was obtained by switching the CI of the activating agent from a  $\text{OTf}^-$  to  $\text{BF}_4^-$ . Due to the less coordinating nature of the latter, increased electrophilicity of the iodine center of the activating agent towards benzhydryl bromide allowed for a more effective conversion increasing the yield from 85% to a staggering 97%.<sup>34</sup> In other examples,<sup>35</sup> a direct coordination by counterions was observed for hypervalent halonium cations in di-arylhonium salts where their positive  $\sigma$ -holes are able to influence the formation of short contacts in the solid state with anions.



**Scheme 2.** A direct CI effect on XB demonstrated. <sup>34</sup>

## 4. Carbocations

Without a doubt, much of the discussion on pentacoordinate carbocations today dates back to ideas pioneered by Nobel laureate George A. Olah.<sup>36,37</sup> To experimentally generate a three-center-4-electron (3c4e) bond of a pentacoordinate system, three methods are typically considered<sup>38</sup> - (i) by coordination of two radicals to an unshared electron pair, or (ii) by coordination of two lone pairs to a vacant p orbital and (iii) by coordination of one lone pair to the antibonding orbital of the sigma bond. The pentavalent  $[\text{NCN}]^+$  carbonium complexes and the halogen bonded  $[\text{NXN}]^+$  systems discussed in this thesis are analogous to each other in that they both have an empty  $p_z$  orbital. Both  $[\text{X}]^+$  of bis(pyridine)halogen(I) complexes and the  $[\text{C}]^+$  center of triphenylcarbenium tetrafluoroborate have an empty and available 'p-hole' prior to complexation, i.e. the two anti-parallel lobes of a vacant  $p_z$ -orbital, that are analogous to the electron depleted  $\sigma$ -hole, and can simultaneously accept electron density donation from the two unshared electrons of the pyridine nitrogens (Figure 6). Thus by filling these p-orbitals, the reactivity of such electrophilic species can be modulated and analyzed.

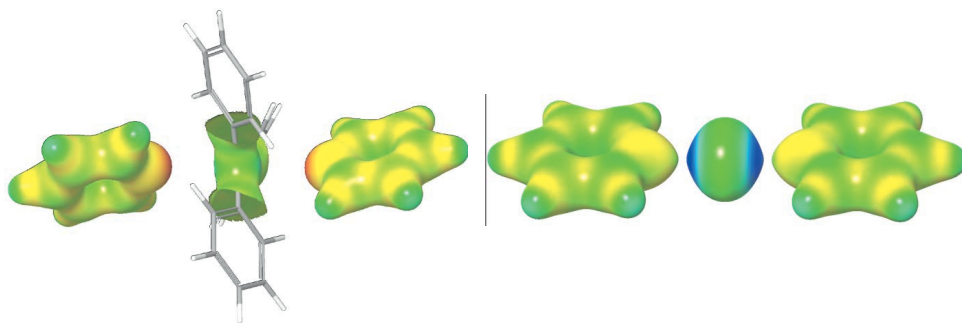


**Figure 6.** The three-center-four-electron bond,  $[\text{N}-\text{C}-\text{N}]^+$ , of hypervalent carbons (left) resembles the isoelectronic three-centered halogen bonds,  $[\text{N}-\text{X}-\text{N}]^+$  (right). The empty p-orbital of the central atom of both complexes possesses two electrophilic regions (blue) that simultaneously receive electrons from two Lewis bases (red), here the nonbonding orbital of two complexing pyridines. The structures shown above were calculated at the M06/MIDIX//M06/LACVP\*\* level and are shown with the contour value 0.08 a.u. and the color ramp 300 (red) 2250 kJ/mol (blue).

For the carbocations, this configuration is normally unstable as the pentacoordinate geometry corresponds to a transition structure rather than a minimum. Under geometrically restrained conditions, there are few reports on pentavalent carbons as an *intramolecular* complex between boron, oxygen and sulfur donors and crystal structures obtained.<sup>39,9</sup> Due to the fundamental impact of the nucleophilic substitution reaction mechanism, the generation of model compounds having a stable *intermolecular* pentavalent carbon has been attempted in order to allow experimental investigation of this high energy configuration under standard laboratory conditions.

## 5. Objectives of this thesis

---

The overall aim of this thesis work was to investigate the moderately strong, non-covalent interactions involved in three-center-four-electron (3c4e) complexes of  $[X]^+$  and  $[C]^+$  species as part of  $[NXN]^+$  or  $[NCN]^+$  systems respectively. The nitrogen containing donors used for the study were either pyridine moieties or its geometrically restricted bidentate analog 1,2-bis(pyridine-2-ylethynyl)benzene.

The specific objectives were to:

- Synthesize  $[NXN]^+$  and  $[NCN]^+$  complexes in order to compare and contrast their geometries.
- Characterize the labile and highly reactive chlorine and fluorine centered halonium ions as part of the  $[NXN]^+$  halogen bonded system.
- Investigate whether counterions influence the geometry of the iodine centered halogen bond using an exceedingly accurate NMR methodology.
- Compare and contrast geometric preferences of tertiary carbocations complexed to pyridines and 1,2-bis(pyridine-2-ylethynyl)benzene donor moieties.
- Verify the ability of these carbocations to form intermolecular pentavalent geometries.





## 6. Chlorine and Fluorine centered XB's (Paper I)

### 6.1 Three center 4 electron

Three-center-4-electron (3c4e) halogen bonds, sometimes also referred to as coordinative halogen bonds,<sup>22</sup> are formed by the simultaneous interaction of an electrophilic halogen  $[X]^+$  with two electron donor functionalities, D. As the halonium ion by itself is a highly reactive species, they are therefore studied here as part of a three center system.<sup>40</sup> In these  $[D\cdots X\cdots D]^+$  complexes, the halogen follows a different electronic configuration prior to complexation than the representation shown in Figure 1. The majority of the complexes discussed herein lack  $\sigma$ -holes but instead comprise of “p-holes”<sup>19</sup> as the electropositive charge of the halonium species is generated by depopulating the  $p_z$  orbital ( $p_x^2 p_y^2 p_z^0$ ) thereby allowing the donors to approach the empty and antiparallel lobes of the halonium from opposite ends (Figure7). The remaining two filled p-orbitals develop a negative belt around the lateral sides of the halonium ion. The electropositive tips are ideally positioned to simultaneously accept electron density donation from the lone pairs of the nitrogens giving rise to the directionality that is typical of XB's. The positively charged  $[X]^+$  can thus be considered as a halogen bond donor capable of forming two halogen bonds simultaneously. An example of such a system is the [bis(pyridine)iodine]<sup>+</sup> complex shown in Figure7.

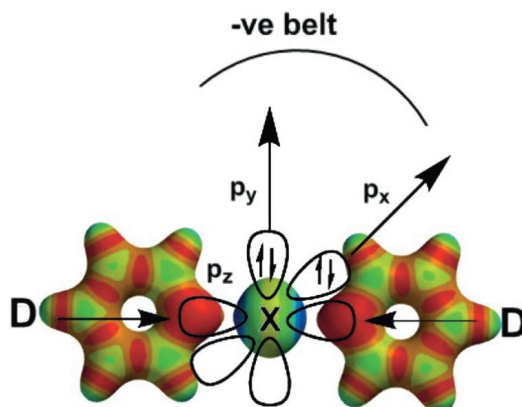


**Figure 7.** The surface electrostatic potential of the [bis(pyridine)iodine]<sup>+</sup> complex. The antiparallel p-holes of I<sup>+</sup> (blue) are separated by an equatorial of neutral charge (yellow). Each p-hole interacts with the nonbonding electron pair of a pyridine nitrogen. The surface was computed on a 0.008 au contour of the electronic density for visualization. Color ranges, in kJ/mol, are as follows: red, less than 350, yellow between 350 and 390, green between 390 and 470, light blue between 470 and 490, and blue greater than 490.

Due to their unconjugated positive charge, halonium ions react readily with nucleophiles and are typically short lived, high energy intermediates in organic reactions. New and stable sources of electrophilic halogens are always desirable as they are considered to be synthetically useful species for I<sup>+</sup> or Br<sup>+</sup> transfer reactions in, for example, halocyclizations,<sup>41</sup> halogenation of alkenes and alkynes.<sup>42</sup> Since positively charged iodine<sup>43-46,40</sup> and bromine are comparatively well documented species,<sup>40,45-46</sup> this chapter aims to show experimental observation of chlorine and fluorine centered halogen bonds by stabilizing these halogens between nitrogen donors and describe their geometries using solution spectroscopy and computational methods (paper I).

## 6.2 Synthesis and NMR of **3c**

[NXN]<sup>+</sup> systems were synthesized using a published procedure employed for analyzing the iodine and bromine centered analogs.<sup>40</sup> We start by generating the precursor [bis(pyridine)silver]<sup>+</sup> complex **2** which undergoes a cation exchange process in the presence of molecular X<sub>2</sub>. The driving force for generating the X<sup>+</sup> species is therefore the precipitation of the silver halide salt, whereas the X<sup>+</sup> is stabilized by getting trapped between the two Lewis basic pyridines (Scheme 3). The AgX that precipitates is removed by centrifugation followed by a transfer of the supernatant to a separate vial under an Ar(g) atmosphere. Addition of hexane to the supernatant yields complexes **3a** and **3b** as solids.



rate than **1** and **2**, which is expected, as it is known<sup>48</sup> to exist as a mixture involved in a rapid equilibrium exchange process.<sup>49</sup> The longitudinal relaxation of **3c** is significantly faster than that of the dynamic  $[\text{NHN}]^+$  complex suggesting that the rapid relaxation rate of **3c** is not due to an exchange process.

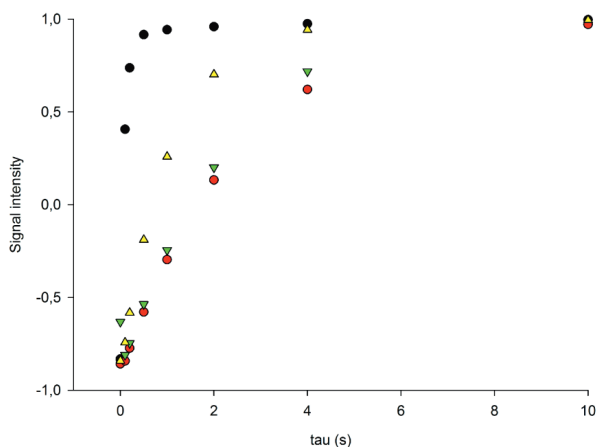


**Figure 8.** The inversion recovery experiment of all 4 different species compared. The data points of bis(pyridine)chloronium triflate **3c** are in black ( $T_1 = 0.08$  s) and those of bis(pyridine)silver(I) triflate **2** in green ( $T_1 = 1.49$  s), pyridine **1** in red ( $T_1 = 1.61$  s) and NHN complex in yellow ( $T_1 = 0.71$  s). The exceptionally rapid relaxation observed for **3c** is the consequence of the quadrupolar moment of chlorine(I).

In addition to inversion recovery experiments, the formation of the chloronium species was further confirmed by comparing its proton and carbon shifts to that of **2**. Fig 9 shows the overlapped  $^1\text{H}$  NMR spectra of the two whereby a considerable shift change is observed when chlorine gas is introduced into the precursor solution. Due to the high reactivity of complex **3c**, upon contact with humidity it decomposes to the corresponding  $[\text{bis}(\text{pyridinium})]^+$  triflate which can be seen as the minor set of broad peaks in the same spectrum. In order to determine whether there are similar dynamic processes occurring within the halogen bonded molecular entity as there is in the hydrogen bonded system, the NMR technique of measuring the temperature dependence of isotopic perturbation of equilibrium (IPE) may be applied. This method allows for distinguishing a single, static symmetric molecule from a pair of rapidly interconverting asymmetric isomers by measuring temperature dependence of the magnitude of equilibrium isotope shift induced by

isotope substitution close to the interaction site. The major advantage of this method is that it succeeds even when the signals coming from the different tautomers are coalesced and become identical to those of a single static structure ( $[\text{N}-\text{X}\cdots\text{N}]^+ \rightleftharpoons [\text{N}\cdots\text{X}-\text{N}]^+$  or  $[\text{N}\cdots\text{X}\cdots\text{N}]^+$ ). However, due to the temperature dependence of the chloronium species, we were unable to perform IPE on **3c**. Its structure was therefore confirmed by computational analysis in addition to NMR.

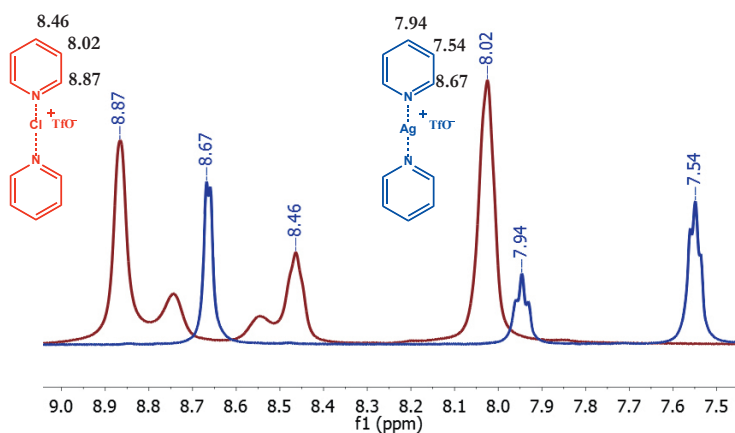
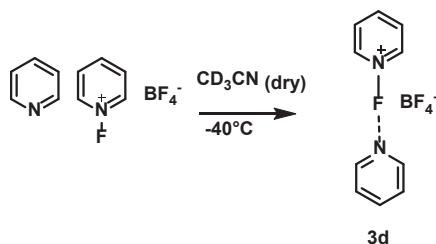


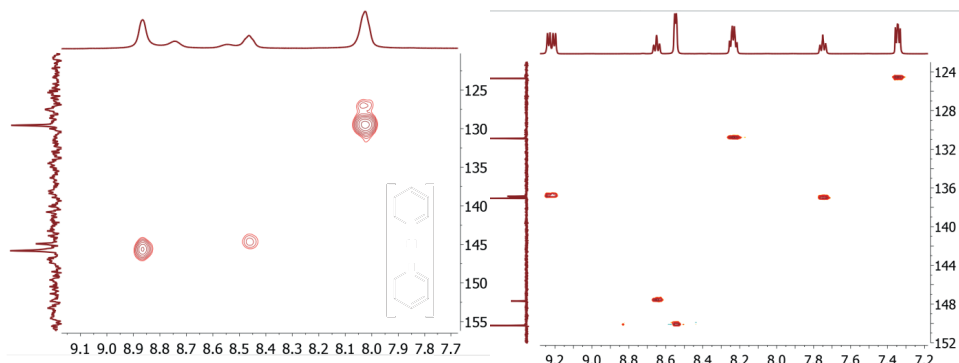
**Fig 9.** Bis(pyridine) chloronium (red) and bis(pyridine)silver (blue). A considerable shift change is observed upon introduction of  $\text{Cl}_2$ . Moisture induced decomposition was also observed and shown as the minor set of peaks (unmarked) in the red spectra.

### 6.3 Synthesis and NMR of 3d

Due to the known hazards associated with the use of  $F_2$  gas, we employed a different strategy towards the generation of an  $[NFN]^+$  complex (Scheme 4). The commercially available *N*-fluoropyridinium tetrafluoroborate salt was dissolved in dry  $CD_3CN$  instead of  $CD_2Cl_2$  due to the poor solubility of ionic species in the latter. Pyridine (1 eq) was carefully added and the resulting shift changes measured. Bearing in mind the choice of solvent, we conducted the experiment at  $-40\text{ }^\circ\text{C}$  since acetonitrile freezes below that. Based on earlier work,<sup>50</sup> it was known that these complexes were unstable at room temperature considering that *N*-fluoropyridinium is an excellent fluorinating agent. In contrast to its iodine, bromine and chlorine centered analogues, complex **3d** gave two distinct sets of signals indicating that its pyridines were in different chemical environments – one set of signals corresponding to a pyridine ring having a strong N-F covalent bond; and another that indicated towards a weaker halogen bond (Table 1, Figure 10). As the temperature was raised, the sample decomposed rapidly generating multiple sets of peaks indicating the progress of chemical reaction and thus the formation of several reaction products.



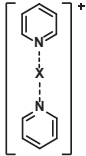
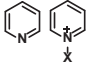
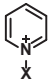
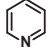
**Scheme 4.** Modified route employed towards generating the fluorine centered complex **3d** due to known hazards associated with  $F_2(g)$



**Figure 10.** HSQC spectra of **3c** and **3d**. The distinct signal separation observed for the asymmetric  $[\text{NFN}]^+$  species (*right*) is in sharp contrast to the symmetric  $[\text{NCIN}]^+$  species (*left*).

Although the change in the nitrogen for the incoming pyridine ring and the fluorine chemical shift of the covalently bound ring are only in the magnitude of 2-3 ppm, [ $^{15}\text{N}$  ( $\delta$  -65.8 to -68.8) and  $^{19}\text{F}$  ( $\delta$  47.0 to 45.9)] these along with a significant reduction in diffusion rate indicates the formation of a weak, halogen bonded complex. *N*-Fluoropyridinium diffuses significantly faster when free and drastically reduces its speed when the second pyridine moiety is introduced (free =  $120.3 \times 10^{-10} \text{ m}^2\text{s}^{-1}$   $\rightarrow$  coordinated =  $41.2 \times 10^{-10} \text{ m}^2\text{s}^{-1}$ ). Although the incoming pyridine ring is still diffusing slightly faster ( $46.7 \times 10^{-10} \text{ m}^2\text{s}^{-1}$ ) than the covalently bound ring, if no interaction occurred at all between them; it would diffuse more independently. The above data are compatible with a weakly interacting mixture of pyridine and *N*-fluoropyridinium tetrafluoroborate and the resulting formation corresponds better to an asymmetric system held together by a conventional, weak halogen bond instead (Table 1). Hence, even though the  $\sigma$ -hole of fluorine is small, at low temperatures, the weak halogen bond of **3d** can be detected.

**Table 1.** Chemical shift changes observed upon formation of **3a-d**

Substance	X	Temp	$\delta\text{N}(\text{ppm})$	$\delta\text{F}(\text{ppm})$	Diffusion rate $D(\text{H})\text{m}^2\text{s}^{-1}$
	I	25°C	-175.1		
	Br	25°C	-142.9		
	Cl	-80°C	n.d.		
	F	-35°C	-122.1	45.9	$41.2 \times 10^{-10}$
			-68.8		$46.7 \times 10^{-10}$
	F	-35°C	-122.1	47.0	$120.3 \times 10^{-10}$
	-	-35°C	-65.8		

## 6.4 Computational optimization

Molecular symmetry is commonly described by potential electrostatic energy curves.<sup>51</sup> The three possible scenarios that the  $[\text{X}]^+$  can adapt are as follows (i) static symmetric - to be centered between the nitrogens having two equal N–X distances or (ii) static asymmetric - have a strong preference to be closer to one nitrogen over the other  $[\text{N}-\text{X}\cdots\text{N}]^+$  or (iii) dynamic asymmetric whereby the halogen can rapidly move between the nitrogens over a shallow energy barrier ( $[\text{N}-\text{X}\cdots\text{N}]^+ \rightleftharpoons [\text{N}\cdots\text{X}-\text{N}]^+$ ). The latter may lead to coalescence of the individual NMR signals coming from the interchanging forms and thus the observation of a single, time-averaged signal is similar to the signal from a static form (Figure 11).



Single energy minima are often correlated with static symmetric geometries corresponding to scenario (i) whereby the nitrogen is equidistant from both donors  $[\text{N}\cdots\text{X}\cdots\text{N}]^+$ . The  $[\text{N}^+-\text{F}\cdots\text{N}]$  system is an example of a static asymmetric scenario (ii) whereby the asymmetry is visible in the  $^1\text{H}$  and  $^{13}\text{C}$  NMR spectrum as two distinct set of signals due to a high energy barrier between the isomeric states.

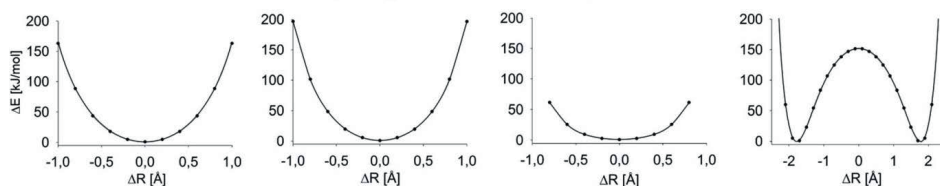


**Figure 11.** The calculated potential energy wells for the bis(pyridine) halonium complexes describing the relationship between their geometry and energy. From left to right: NIN (**3a**), NBrN (**3b**), NCIN (**3c**) and NFN (**3d**).

To confirm the experimentally determined symmetries, the geometries of the  $[\text{NXN}]^+$  complexes **3a-d** were evaluated by computational methods (Figure 12). Geometry optimizations were performed on the DFT level (B3LYP) applying a dichloromethane solvent model using the B3LYP functional.<sup>1</sup> The symmetric NXN systems are predicted to be 16-20 kJ mol<sup>-1</sup> more stable than the corresponding asymmetric N-X $\cdots$ N complexes and the creation of a symmetric NFN bond would require an overall 138 kJ mol<sup>-1</sup> energy investment. Accordingly, **3d** does not form a symmetric complex and **3c** does.

<sup>1</sup>Calculations were performed by Assoc. Prof. Jürgen Gräfenstein and former MSc student Marcus Reitti

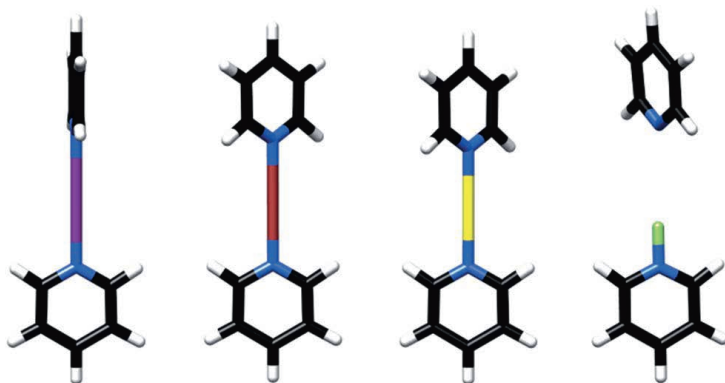


**Figure 12.** DFT geometry optimization (B3LYP/LANL08d) predicted static, symmetric [N–X–N]<sup>+</sup> halogen bonds for the iodine, bromine and chlorine centered bis(pyridine)halonium complexes shown from the left to the right, whereas an asymmetric arrangement for fluorine. Iodine is shown in violet, bromine in red, chlorine in yellow and fluorine in green.

## 6.5 Summary Paper I

In conclusion, DFT confirms NMR observation that much like the heavier halogens, the chlorine centered [NCIN]<sup>+</sup> complex also forms a symmetric geometry when trapped between pyridine moieties. The [NFN]<sup>+</sup> system is asymmetric, analogous to the [N–H⋯N]<sup>+</sup> hydrogen bond<sup>52,53</sup> but due to a high energy barrier between the donors, isomerization is disfavored.

## 7. Counterion Effects on XB Symmetry (Paper II)

The solid state structure as detected by X-ray diffraction does not necessarily represent the solution geometry. Therefore, a disordered environment, such as that in solution, can induce asymmetry whereas the same system can display a symmetric arrangement in a more restricted, ordered environment such as in crystal structures. Although slight differences in N-X distances of positively charged bromine(I)<sup>45-46</sup> and iodine(I) species<sup>54,55,56</sup> between nitrogen donors were reported earlier in solid state, their symmetries were not verified in solution. As part of our ongoing investigation for gaining an improved understanding of 3c4e halogen bonding in solution,<sup>57,40a-c</sup> counterion effects were investigated to see whether the geometry of the [bis(pyridine)iodine]<sup>+</sup> system could potentially be influenced. The counterion may coordinate to the [NIN]<sup>+</sup> system in one of three ways: (a) it may coordinate strongly to one pyridine ring over the other and induce asymmetry, or (b) symmetrically orient itself from both rings and not affect the geometry at all, or (c) coordinate to one ring but not induce any symmetry changes in the [NXN]<sup>+</sup> bond. Depending on the orientation, the complex may have varying reactivities as the halogen could potentially be transferred with more ease from one system over the other in the presence of an olefin for example. A schematic representation of the idea is shown in Figure 13.

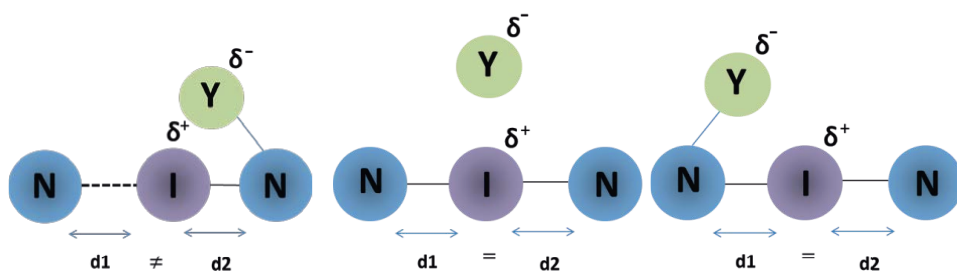


**Figure 13.** The three different scenarios that could arise from counterion coordination. *Left.* CI coordination leads to distortion of linearity. *Middle* CI does not have a preference for one over the other. *Right* Weak CI coordination does not affect N-I distances.

In order to elucidate whether counterions can influence the symmetry of **3a** ( $[\text{N}-\text{I}\cdots\text{N}]^+ \rightleftharpoons [\text{N}\cdots\text{I}-\text{N}]^+$ ) the isotopic perturbation of equilibrium method was utilized following published procedures.<sup>57b, 57c</sup>

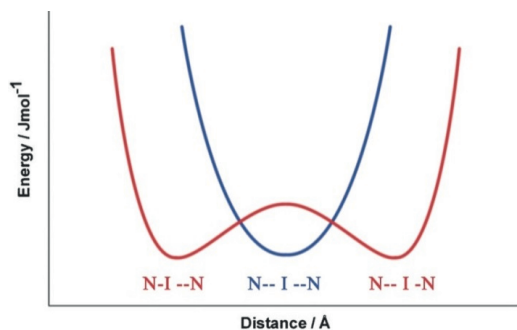
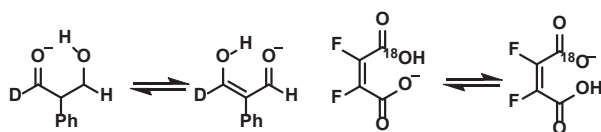


**Figure 14.** Schematic potential energy curves for a static symmetric species (blue) and that of rapidly interconverting, asymmetric one (red). If the exchange between them is fast enough, signal coalescence arises and the two appear to be exactly the same by NMR due to signal coalescence.

## 7.1 Isotopic Perturbation of Equilibrium (IPE)

IPE, a principle based on an isotope induced perturbation of equilibrium, requires the selective introduction of an isotope that results in a chemical shift difference called the isotope effect in an isotopolog mixture. The choice of isotope varies but most common is the substitution of a  $^1\text{H}$  with  $^2\text{H}$  or  $^{16}\text{O}$  with  $^{18}\text{O}$ .<sup>58</sup> This technique was successfully utilized to elucidate the asymmetry in intramolecular NHN and OHO hydrogen bonds<sup>59</sup> for example (Scheme 5).<sup>60,49a</sup> It should be noted that the labeling should take place with an isotope that is of similar size to that which is being substituted. Introduction of the isotope itself should not cause any overall major structural changes therefore inadvertently inducing asymmetry. The isotope is selectively introduced close to the interaction site causing vibrational energy changes in a molecule which eventually affect the observed vibrationally averaged

NMR parameters.<sup>61</sup> This asymmetric introduction of the isotope will perturb any rapid equilibrium process the system may be undergoing.



**Scheme 5.** Examples of geometries evaluated by using IPE.

For the isotopologs discussed in this thesis, the labelling is introduced into the C2 position of **3a** by replacing a  $^1\text{H}$  with a  $^2\text{H}$ . Following the Born-Oppenheimer approximation which provides a theoretical description of isotopic substitution on molecular properties,<sup>62</sup> the two participants of the equilibrium process will have differences in their zero point energies (ZPE) as the ZPE for a C-H bond is slightly larger than that of a C-D.<sup>63</sup> ZPE is inversely proportional to the square root of mass, therefore the slightly heavier deuterium will be lower in energy.<sup>64</sup> Equilibrium isotope effects are temperature dependent and are therefore possible to detect as the magnitude of the isotope shift will have a large temperature dependency. Since this NMR technique requires  $^{13}\text{C}$  analysis of an isotopolog mixture; two sets of signals are observed - one from the deuterated and the other from the non-deuterated analog for the same position. Figure 15 demonstrates the signal separation that is observed when an isotopolog mixture is present. The pair of signals arising from a selected position of the pyridine ring is shown as an example, but isotope shifts are detectable on every carbon of the pyridine ring. The C2 and C3 positions give the largest isotope shifts being closest to the site of substitution. Additionally, there is some loss of intensity for the C2 signal (one bond away from D) due to reduced NOE as a result of a proton substitution to deuterium making C3 (two bonds away from D) an easy and reliable position to measure the magnitude of isotope shifts on.

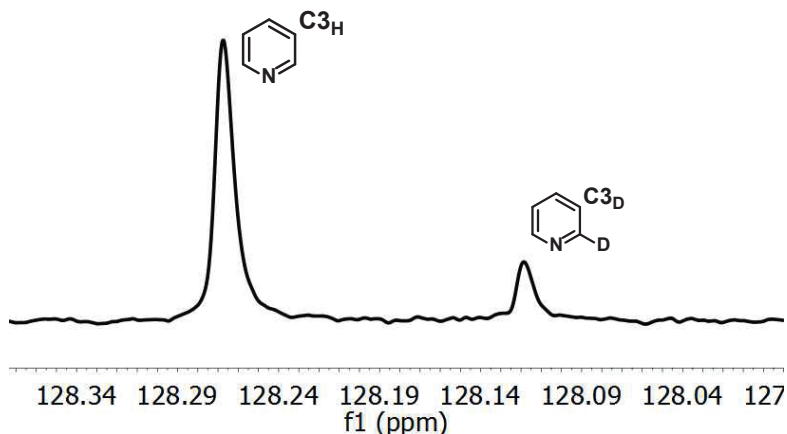


**Figure 15.**  $^{13}\text{C}$  chemical shift difference that arises in an isotopologue mixture,  ${}^n\Delta_{\text{obs}}$  for the C3 position in a sample containing deuterated and non-deuterated pyridines

This shift difference, or the isotope effect, is described as  ${}^n\Delta_{\text{obs}}$ , where  $n$  is the number of bonds between the position of substitution and the investigated carbon. Therefore as  $n$  increases,  ${}^n\Delta_{\text{obs}}$  decreases.  ${}^n\Delta_{\text{obs}}$  has two factors contributing to it; an intrinsic effect,  ${}^n\Delta_0$  which arises simply due to the substitution by an isotope and an equilibrium effect,  ${}^n\Delta_{\text{eq}}$  which manifests *only* if there are equilibrium processes occurring within the system (eq 1).

$${}^n\Delta_{\text{obs}} = \delta_{\text{C(D)}} - \delta_{\text{C(H)}} = {}^n\Delta_0 + {}^n\Delta_{\text{eq}} \quad (1)$$

Since  ${}^n\Delta_{\text{eq}}$  arises from exchange processes occurring within the system, the magnitude of  ${}^n\Delta_{\text{eq}}$  depends on the equilibrium constant  $K$  of the exchange process as denoted by

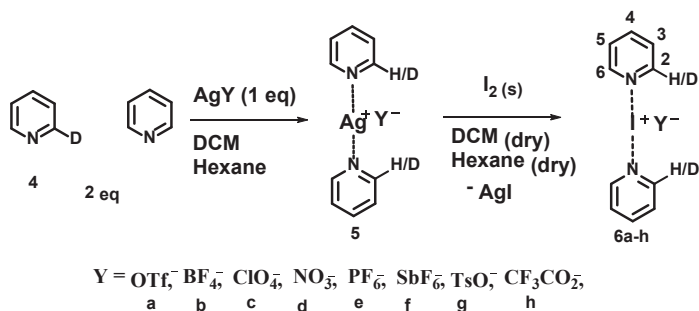
$${}^n\Delta_{\text{eq}} = D(K-1)/[2(K+1)] \quad (2)$$

where  $D$  denotes the chemical shift difference between the signals of the isomeric forms. The equilibrium constant,  $K$ , is temperature dependent according to the

van't Hoff equation,<sup>65</sup> therefore so is  ${}^n\Delta_{\text{eq}}$ . The intrinsic effect will manifest itself in both the static symmetric and rapidly equilibrating forms since it occurs due to the substitution of a  ${}^1\text{H}$  with  ${}^2\text{H}$  and is also temperature dependent as a result of solvent polarity changing slightly with temperature therefore modulating the electron density of the nitrogen lone pair of the pyridine.<sup>66</sup> However, the effect diminishes rapidly with increasing  $n$ . The main difference between  ${}^n\Delta_{\text{eq}}$  and  ${}^n\Delta_0$  therefore lies in that; the magnitude of the isotope shift from equilibrating systems has a significantly larger temperature dependency than those from static geometries as the former is a reflection of the temperature induced alteration of an equilibrium process.

## 7.2 Synthesis, Analysis & Variable Temperature (VT) NMR

Investigated isotopolog mixtures were generated following a procedure similar to that for **3a-c** with some modifications (Scheme 6). By adding the silver salt into a mixture of deuterated and non-deuterated pyridines, the precursor [bis(pyridine)Ag]<sup>+</sup> complex **5** was synthesized. The CIs were chosen such that they varied according to size and coordination strength and were introduced at this stage by varying the Ag(I) salt. Before addition of the halogen, the precursor was dried thoroughly to avoid any moisture induced decomposition. Silver halide precipitated out as the DCM solution of I<sub>2</sub> was added. The solid was centrifuged and the supernatant transferred to a separate pre-dried vial. The electrophilic I<sup>+</sup> species that formed was trapped between the two donors thereby generating **6a-h**. Addition of dry hexane to the supernatant yielded the desired complex as an isotopolog mixture.



**Scheme 6.** Generation of isotopologue mixtures for IPE studies

This mixture was then dissolved in dry  $\text{CD}_2\text{Cl}_2$  and  $^{13}\text{C}$   $\{^1\text{H}, ^2\text{H}\}$  spectra acquired from  $25^\circ\text{C}$  to  $-40^\circ\text{C}$  with  $10^\circ\text{C}$  intervals. In order to obtain higher sensitivity and thereby increase the reliability of the measurement, the spectra were acquired with simultaneous proton and deuterium decoupling. If decoupling were not applied, the signal to noise ratio would be significantly reduced due to  $^{13}\text{C}$ - $^2\text{H}$  ( $J_{\text{CD}}$ ) couplings resulting in the signals coming from the deuterated analog to be split into triplets. This is illustrated in the superimposed spectra below (Figure 16) whereby the higher intensity obtained as a consequence of decoupling is demonstrated.

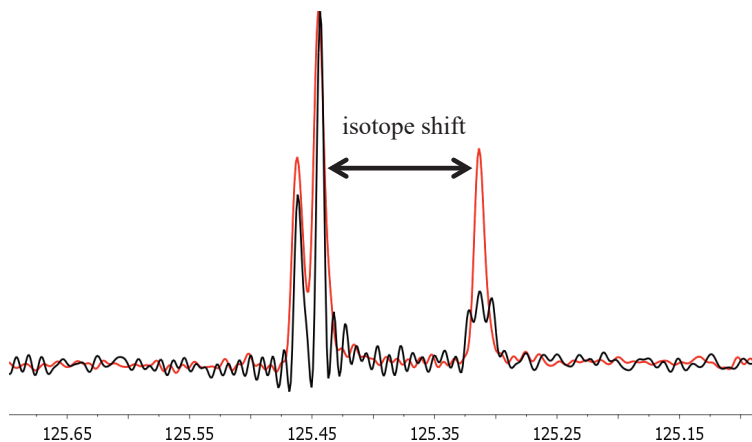
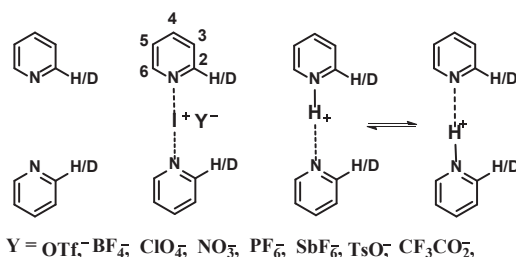


**Figure 16.** Increasing signal intensity and thereby reliability of the measurement by decoupling. Measurement in black is with  $^1\text{H}$  decoupling. Same spectra in red with simultaneous decoupling on  $^1\text{H}$  and  $^2\text{H}$  frequencies.



The temperature coefficients of the isotope shifts were acquired from the slope of  ${}^n\Delta_{\text{obs}}$  vs. reciprocal temperature ( $1/T$  (K)) plots (Table 2). For each of the CIs, isotope shifts were measured for each carbon of the pyridine ring at each temperature and the sum of the isotope shifts,  $\Sigma\Delta_{\text{obs}}/T$  compared. For simplicity, Table 2 shows the isotope effect for only the C3 position and the summation over the whole complex for comparison. The  $\Delta_{\text{obs}}/T$  for each position are given in detail in paper II. For a complete and thorough comparison, the geometries are discussed in relation to two reference systems: (i) that of free pyridines as the static reference (no dynamics) providing estimates for the intrinsic isotope shifts i.e.  $\Delta_{\text{obs}} = {}^n\Delta_0$ ; and (ii) the [bis(pyridine)hydrogen] $^+$  complex which has already been established to be asymmetric both in solution and in the solid state<sup>67</sup> and therefore generates, in addition to the intrinsic, the equilibrium component as well;  $\Delta_{\text{obs}} = {}^n\Delta_0 + {}^n\Delta_{\text{eq}}$ . Its asymmetry becomes apparent by  ${}^1\text{H}$  NMR without any labeling at  $-150^\circ\text{C}$ .<sup>67</sup>



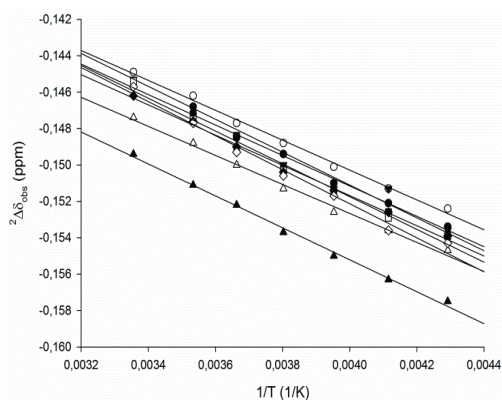
**Scheme 7.** The different systems compared by IPE

Since the studied systems show an overall small temperature dependency in comparison to the asymmetric  $[\text{NHN}]^+\text{OTf}^-$ , we conclude that complexes **6a-h** occur as static, symmetric species in solution with the  $\text{I}^+$  equidistant from the two nitrogens. Their  $\Sigma\Delta_{\text{obs}}/T$  shifts are more similar to those of free pyridines measured over the same temperature range. The above observations concur well with previously reported high energetic gain upon the formation of a symmetric  $[\text{N}\cdots\text{I}\cdots\text{N}]^+$  halogen bond.<sup>68</sup> Noteworthy to reiterate is that IPE experiment allows us to reproduce that the  $[\text{NHN}]^+$  system is indeed asymmetric but without having

to cool the spectrometer to  $-150^{\circ}\text{C}$ .<sup>48</sup> Dynamic systems possess an equilibrium isotope effect that has a large temperature dependency, well reflected in the  $\Sigma\Delta_{\text{obs}}/T$  data for the  $[\text{NHN}]^+$  system. If the the halogen bonded systems **6a-h** were involved in an equilibrium effect, their  $\Sigma\Delta_{\text{obs}}/T$  would be expected to be larger.

**Table 2.** (*Left*) Temperature coefficients (ppm K) of the isotope shifts of **6a-h** observed for  $\text{CD}_2\text{Cl}_2$  solutions from  $25^{\circ}\text{C}$  to  $-40^{\circ}\text{C}$ . (*Right*) Isotope shift  $^2\Delta_{\text{obs}}$  vs reciprocal temperature plot

Anion	$^2\Delta_{\text{obs}}$	$\Sigma\Delta_{\text{obs}}/T$ (ppm $\times\text{K}^{-1}$ )
Pyr/Pyr- <i>d</i>	-5.0	15.0
$\text{BF}_4^-$	-8.4	18.2
$\text{ClO}_4^-$	-8.3	17.8
$\text{PF}_6^-$	-8.9	19.0
$\text{SbF}_6^-$	-9.0	19.4
OTf	-8.5	18.4
$\text{TsO}^-$	-8.1	14.2
$\text{NO}_3^-$	-8.0	17.2
$\text{CF}_3\text{CO}_2^-$	-8.8	20.6
$\text{CF}_3\text{CO}_2^-$ <sup>a</sup>	-9.4	20.0
$[\text{NHN}]\text{OTf}$	-9.8	34



<sup>a</sup>The counterion was scavenged using  $\text{Bn}12\text{BU}[6]$  thus providing the naked  $[\text{bis}(\text{pyridine})\text{iodine}]^+$

### 7.3 Scavenging the CI

In addition to determining the effect on the symmetry of  $[\text{NXN}]^+$  complexes upon varying the CI, we further investigated how they behave in the absence of the CI as tight ion pairing of the counterion to the cationic  $[\text{NIN}]^+$  complex was observed for their  $\text{CD}_2\text{Cl}_2$  solution by diffusion NMR spectroscopy (DOSY). Does the  $[\text{NIN}]^+$  complex hold its static, linear arrangement independent of the CI? By scavenging the CI with bambusuril  $\text{Bn}_{12}\text{BU}[6]$ ,<sup>69</sup> an anion scavenger that has high affinity towards tetrafluoroborate and triflate anions, we analyzed the  $[\text{NIN}]^+$  complex in the absence of its CI. In order to ensure that the CI was completely removed, we added a slight excess of bambusuril to the  $\text{CD}_2\text{Cl}_2$  sample of **6b** and consequently measured the temperature dependence of its isotope effects. A clear cross peak in a F,H-HOESY spectrum between the protons of the bambusuril and the fluorine of  $\text{BF}_4^-$  ensured that the cationic complex was completely detached from its CI. A comparison of the isotope shifts obtained for this “counterion free” system with those of the static symmetric and dynamic asymmetric references showed that the [bis(pyridine)iodine]<sup>+</sup> system prefers to be linear even in the absence of a CI and that its geometry holds true independent of the CI. (Table 2)

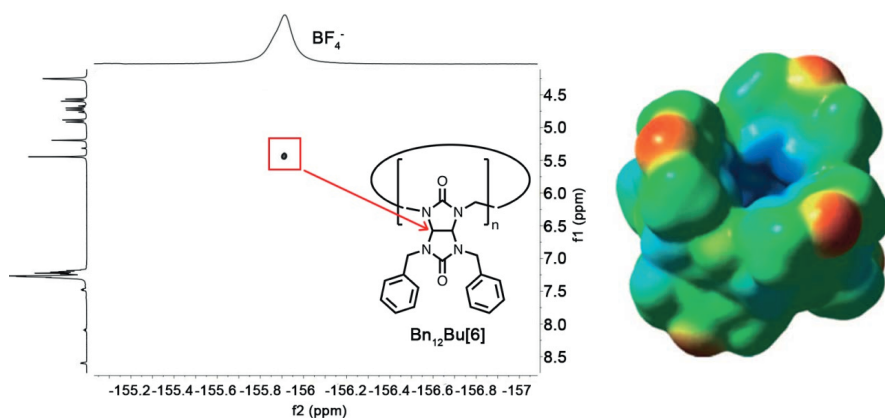



Figure 17. HOESY showing crosspeak between bambusuril protons and the  $\text{BF}_4^-$

In addition to the measured isotope shifts, further confirmation that the [NIN]<sup>+</sup> skeleton experienced no change upon scavenging the CI was obtained from the  $\delta^{15}\text{N}$  shifts. As shown in Table 3 the nitrogen shift of the system before and after remained completely unaffected. The diffusion rate of the complexes demonstrates that tight ion pairing was observed before addition of the scavenger. After the addition of the scavenger, the anion and bambusuril diffuse with the same rate, i.e. are complexed, whereas the cationic complex diffuses independently and faster than the bambusuril-anion complex.

**Table 3.** Translational diffusion coefficients, measured by <sup>1</sup>H and <sup>19</sup>F NMR detection and <sup>15</sup>N NMR chemical shifts before and after bambusuril addition

		$D(\text{cation})$ $\times 10^{-10} \text{ (m}^2\text{s}^{-1}\text{)}$	$D(\text{anion})$ $\times 10^{-10} \text{ (m}^2\text{s}^{-1}\text{)}$	$\delta(^{15}\text{N})$ (ppm)
	$\text{BF}_4^-$	16.8	16.4	-175.1
	CI free	9.4	6.0	-175.5
	$\text{Bn}_{12}\text{BU}[6]$		5.8	

## 7.4 XB in the solid state & *in silico* (DFT)

Single crystals were obtained for the nondeuterated precursor **5** and **6a-g**. X-ray analyses verified that the iodine centered **6** prefers a linear, symmetric bis-coordinated geometry in the solid state regardless of the nature of the CI.<sup>2</sup> The CI has a negligible influence on the N-I bond length, <0.2%, and coordinates weakly. Importantly, as shown in Figure 18, although the CI is closer to one pyridine ring over the other, it does not induce any distortion to the symmetry of the halogen bonded complexes. In contrast, the silver(I) centered precursor displays a significantly different trend and forms intricate networks with the more strongly coordinating CI's.<sup>70</sup>

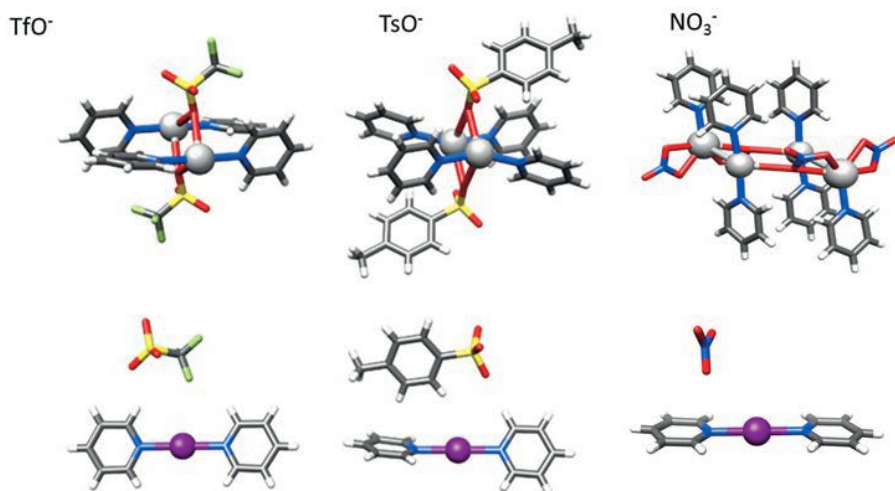


**Figure 18.** (Top) Networks generated by a direct CI coordination to the Ag center. (Bottom) Regardless of the CI, the [NIN]<sup>+</sup> linearity remains unaffected.

<sup>2</sup>Calculations were performed by Assoc. Prof. Jürgen Gräfenstein and former MSc student Marcus Reitti

Additionally, computationally predicted distances and angles confirm those measured in the solid state and confirm the experimental findings (Table 4). Both X-ray data and computation shows that the N-I bond length within the [NIN]<sup>+</sup> complex is virtually unaffected by the CI and the N-I-N bond angle shows only minor variations remaining overall linear.

**Table 4.** Computationally predicted and X-ray crystallographically determined N-I bond distances and N-I-N bond angles

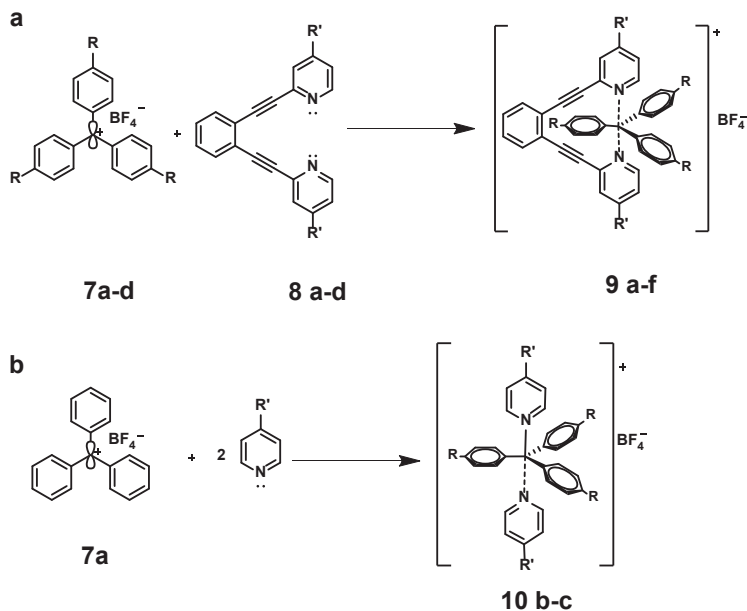
Anion	Computationally predicted distances and angles			X-ray crystallographic distances and angles		
	r(N-I) <sub>1</sub> (Å)	r(N-I) <sub>2</sub> (Å)	σ (N-I-N) (°)	r(N-I) <sub>1</sub> (Å)	r(N-I) <sub>2</sub> (Å)	σ (N-I-N) (°)
BF <sub>4</sub> <sup>-</sup>	2.301	2.301	178.0	2.260(3)	2.260(3)	180.0
ClO <sub>4</sub> <sup>-</sup>	2.301	2.301	175.8	2.257(2)	2.257(2)	180.0
PF <sub>6</sub> <sup>-</sup>	2.303	2.301	178.8	2.268(2)	2.268(2)	180.0
SbF <sub>6</sub> <sup>-</sup>	2.302	2.302	179.2	2.252(3)	2.252(3)	180.0
OTf	2.301	2.300	178.0	2.246(8)	2.261(7)	178.0(3)
TsO <sup>-</sup>	2.301	2.300	177.8	2.241(3)	2.268(3)	178.75(8)
NO <sub>3</sub> <sup>-</sup>	2.303	2.303	179.0	2.250(4)	2.250(4)	180.0
CF <sub>3</sub> CO <sub>2</sub> <sup>-</sup>	2.302	2.298	177.4	-	-	-

## 7.5 Summary Paper II

In conclusion, the counterion does not influence the halogen bond geometry. Even in the absence of the counterion, the much preferred [N•••I•••N]<sup>+</sup> linearity holds true. The symmetry of complexes possessing different CIs was verified by IPE, X-ray and DFT, and all different methods concur. The counter ion does not coordinate directly to iodine(I) in these complexes. Despite high similarities, the analogous transition metal complexes that have Ag(I) in the centrum allow for direct CI coordination to the metal centre and generate intricate networks in the solid state.

## 8. Pentavalent Carbonium Ion in Solution (Manuscript III)

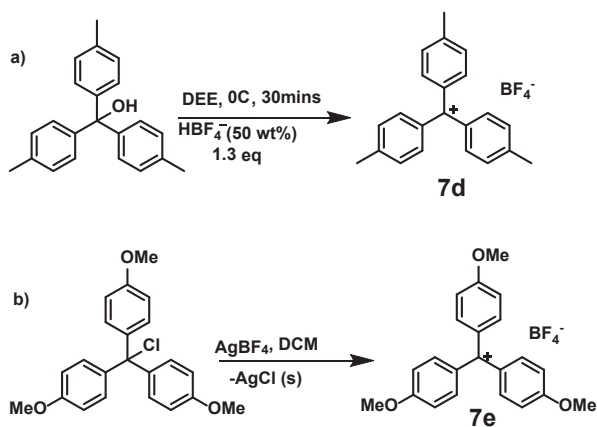
Similar to the cationic halogen,  $[X]^+$ , held in position by two N-X halogen bonds in 3c4e complexes, the carbenium carbon,  $[C]^+$ , of triphenylcarbenium tetrafluoroborate **7** has an empty  $p_z$ -orbital that possesses ‘p-holes’. This p-orbital is capable of simultaneously forming two N-C bonds upon overlapping with the nonbonding orbital of bis(pyridine-2-ylethynyl)benzene **8**. The two nitrogen donors of **8** are positioned at an optimal distance and in ideal orientation to provide orbital overlap and is hence expected to form bonds possessing a partial covalent character,<sup>71</sup> thereby converting the trivalent carbenium of **7** into a pentavalent carbonium in **9** (Scheme 8). If thermodynamically stable, such a complex will be analogous to the transition state of  $S_N2$  reactions and may be useful as a model system.



**Scheme 8.** Syntheses of complexes **9a-f** and **10b-c**, where R = H (a-c), Me (d), OMe (e), NMe<sub>2</sub> (f), R' = CF<sub>3</sub> (a), Me (b), H (c-f).

## 8.1 Synthesis

Compound **8** and its substituted analogs were synthesized following a previously published procedure.<sup>72</sup> Pyridine, 4-picoline, **7a** and **7f** were commercially available, whereas **7d** and **7e** were synthesized from their triaryl alcohol and triaryl halide precursors, respectively (Scheme 9).<sup>73</sup> To generate complexes **9a-f** (Scheme 8), **7a-f** and donors **8a-d** (1:1) were mixed at room temperature under dry conditions in an NMR tube, using dry CD<sub>2</sub>Cl<sub>2</sub> as solvent. For the generation of **10 b-c** (Scheme 8), two equivalents of dried pyridine or picoline were added to the CD<sub>2</sub>Cl<sub>2</sub> solution of triphenylcarbenium tetrafluoroborate, **7a**. As mentioned earlier, <sup>15</sup>N NMR has an inherently wide chemical shift range, ca 800 ppm, and it is expected to provide large, easy to detect chemical shift changes upon formation of weak molecular complexes in which a nitrogen acts as a Lewis base.<sup>71b, 74</sup> Due to its proven applicability, <sup>15</sup>N NMR was applied here as the primary tool to detect the formation of analogous [N⋯C⋯N]<sup>+</sup> complexes.



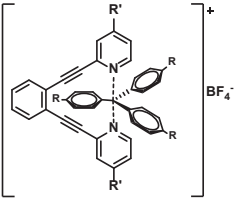
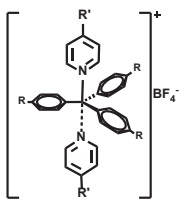
Scheme 9. Generation of cations **7d** and **7e**



## 8.2 NMR

The observation of a single set of  $^{15}\text{N}$  NMR signals for **9a-f** suggests the formation of complexes in which the trityl carbon is equally strongly bound to both Lewis basic nitrogens (Table 5, full table in manuscript III). Accordingly, the  $^{15}\text{N}$  NMR chemical shift change observed on the bidentate donor is accompanied by a large  $^{13}\text{C}$  NMR chemical shift change of the carbenium carbon (Table 5), supporting the formation of an  $[\text{N}\cdots\text{C}\cdots\text{N}]^+$  type complex. Following literature conventions,<sup>75</sup>  $\delta_{\text{coord}}$  is defined as the chemical shift difference of the complex and the free form, that is  $\delta_{\text{coord}} = \delta_{\text{complex}} - \delta_{\text{free}}$ . Whereas bidentate ligands **8a-d** promote formation of a symmetric  $[\text{N}\cdots\text{C}\cdots\text{N}]^+$  complex, the mono-dentate Lewis bases pyridine and picoline form asymmetric ion pairs with **7a** as indicated by the observation of two sets of  $^{15}\text{N}$  NMR chemical shifts for **10b-c** (Table 5). The coordination shifts,  $\delta^{15}\text{N}_{\text{coord}}$ , of the latter complexes suggests that one of the nitrogens form a strong, presumably covalent bond to the carbenium carbon of **7a**, whereas the other nitrogen is involved in a weaker secondary interaction. The magnitude of the observed chemical shift changes are expected to reflect the electron density alteration of the studied complexes, even if they do not necessarily correlate with bond strength.<sup>75</sup> Upon decreasing the electron deficiency of the carbenium carbon, **9c**→**f**, smaller  $\delta^{15}\text{N}_{\text{coord}}$  and  $\delta^{13}\text{C}_{\text{coord}}$  are detected (Table 5) that may be due to a gradual weakening of the  $[\text{N}\cdots\text{C}\cdots\text{N}]^+$  interaction upon decreasing the nucleophilicity of the carbenium carbon. The strong electron donating  $\text{NMe}_2$  functionality of **7f** efficiently decreases the electrophilicity of the carbenium carbon, likely via hyperconjugation, resulting in undetectably small  $\delta^{15}\text{N}_{\text{coord}}$  and  $\delta^{13}\text{C}_{\text{coord}}$  and thus preventing complex formation. For complex **9e**, weak complex formation is reflected in  $\delta^{15}\text{N}_{\text{coord}}$ , whereas no  $\delta^{13}\text{C}_{\text{coord}}$  is seen, revealing that  $^{15}\text{N}$  NMR is a more sensitive tool for detection of  $[\text{N}\cdots\text{C}\cdots\text{N}]^+$  complex formation than  $^{13}\text{C}$  NMR. Increasing electron density of the Lewis basic nitrogen of the bidentate ligand, **8a** < **8c** < **8b**, is associated with an increase of  $\delta^{15}\text{N}_{\text{coord}}$ , that is **9a** < **9c** < **9b**, whereas  $\delta^{13}\text{C}_{\text{coord}}$  remains virtually unaltered. The weak electron donating effect of a 4-Me substituent does not have a large influence on the coordination shifts as reflected by the comparable  $\delta^{15}\text{N}_{\text{coord}}$  and  $\delta^{13}\text{C}_{\text{coord}}$ , of **9b** and **9c** as well as **10b** and **10c**.

**Table 5.**  $^{15}\text{N}$  and  $^{13}\text{C}$  coordination shifts of carbenium complexes

	R, R'	$\delta^{15}\text{N}_{\text{coord}}$ (ppm)	$\delta^{13}\text{C}_{\text{coord}}$ (ppm)	
	<b>9a</b>	H, CF <sub>3</sub>	-28.1	110.2
	<b>9b</b>	H, Me	-82.0	110.2
	<b>9c</b>	H, H	-79.5	109.8
	<b>9d</b>	Me, H	-45.5	123.0
	<b>9e</b>	OMe, H	-16.0	0.0
	<b>9f</b>	NMe <sub>2</sub> , H	0.4	0.0
	<b>10b</b>	H, Me	-86.5	122.1
	<b>10c</b>	H, H	-86.3	121.0

In line with expectation, upon mixing **7a** with 1,2-bis(phenylethynyl)benzene, an analogue of **8c** but without any Lewis basic nitrogen, no  $^{13}\text{C}$  NMR chemical shift alteration on **7a** could be observed corroborating that the interaction seen for **9a-f** involves the nitrogens. As an additional control, the  $^{15}\text{N}$  NMR shift of **8c** was measured in the presence of tri-*p*-tolylmethanol. This resulted in no nitrogen chemical shift alteration of **8c**. The two control experiments confirm that the large  $\delta^{15}\text{N}_{\text{coord}}$  and  $\delta^{13}\text{C}_{\text{coord}}$  observed for **9c** cannot be due to moisture-induced decomposition of **7a** and subsequent hydrogen bonding of triphenylmethanol to **8c**. Whereas bidentate ligands **8a-d** promote formation of a symmetric  $[\text{N}\cdots\text{C}\cdots\text{N}]^+$  complex, the monodentate Lewis bases pyridine and picoline form asymmetric ion pairs with **7a** as indicated by the observation of two sets of  $^{15}\text{N}$  NMR chemical shifts for **10b-c** (Table 5, Figure 19). The coordination shifts,  $\delta^{15}\text{N}_{\text{coord}}$ , of the latter complexes suggest that one of the nitrogens forms a strong, presumably covalent bond to the carbenium carbon of **7a**, whereas the other nitrogen is involved in a weaker secondary interaction.

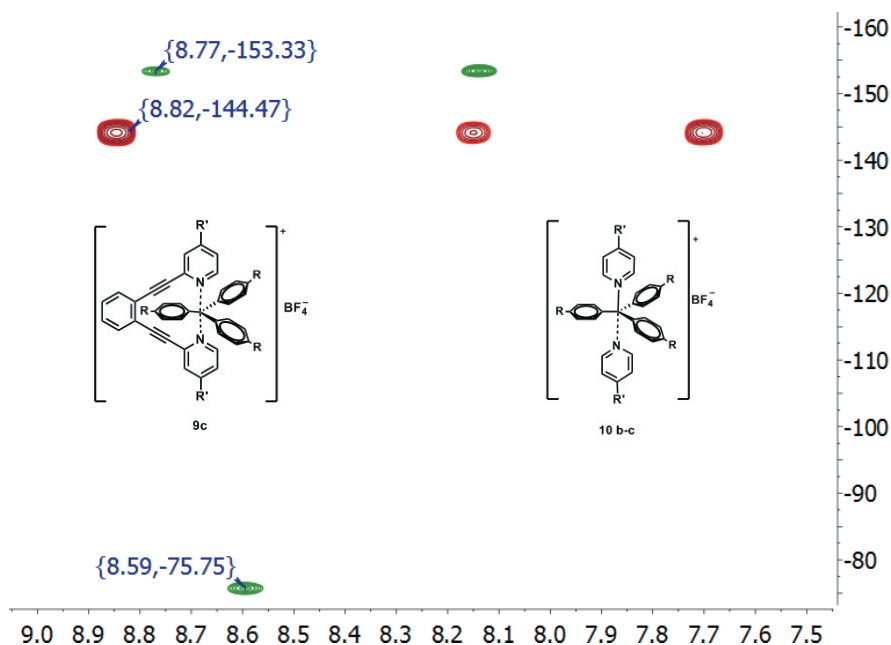


**Figure 19.** Superimposed  $^1\text{H}$ ,  $^{15}\text{N}$  HMBC spectra of complexes **9c** (red) and **10c** (green) acquired in  $\text{CD}_2\text{Cl}_2$  solution at room temperature. Whereas **9c** shows a single set of NMR signals suggesting equally strong coordination of the carbenium ion to both nitrogens, **10c** has an asymmetric structure with a strongly and a weakly coordinating nitrogen revealed by two sets of signals.

Hence, the bidentate Lewis base **8c** is capable of stabilizing a reactive carbenium ion **7a** that rapidly reacts with its monodentate analogue. Strong complexation for **9c** was also supported by the comparable translational diffusion coefficients of **7a** ( $11.5 \times 10^{-10} \text{ m}^2\text{s}^{-1}$ ) and **8c** ( $13.8 \times 10^{-10} \text{ m}^2\text{s}^{-1}$ ) of the formed complex. The diffusion coefficients of **7a** and one of the pyridines ( $\delta^{15}\text{N}_{\text{coord}} -86.3 \text{ ppm}$ ) of complex **10c** are similar ( $9.8 \times 10^{-10} \text{ m}^2\text{s}^{-1}$  and  $9.4 \times 10^{-10} \text{ m}^2\text{s}^{-1}$ ), indicating that these are connected and diffuse together, whereas the second weakly complexing pyridine ( $\delta^{15}\text{N}_{\text{coord}} -8.8 \text{ ppm}$ ) has a diffusion coefficient ( $25.6 \times 10^{-10} \text{ m}^2 \text{ s}^{-1}$ ) that indicates that this pyridine moves independently of **7a** in solution.

### 8.3 Diels-Alder (DA) Kinetics

Triphenyl carbenium ions are powerful Lewis acid catalysts that were used, for example, to facilitate Diels-Alder reactions.<sup>76</sup> Such reactions do not proceed in the absence of a catalyst, whereas upon activation with 0.5 mol% triphenylcarbenium **7a** they give high conversion within 30 min.<sup>76</sup> Therefore to provide additional evidence for the formation of a strong  $[N\cdots C\cdots N]^+$  complex in **9c**, we monitored the progress of two reactions by acquiring the  $^1\text{H}$  NMR integrals of the starting material and the product using their well-separated aldehyde protons as reporter nuclei. In Figure 20 a, the Diels-Alder reaction progresses with second order rate in the presence of **7a**. However, when **9c** is added in which a carbenium ion with an empty p-orbital capable of acting as Lewis acid is converted into a carbonium, the reaction did not give any conversion. This confirms the strong complexation of **7a** to **8c**. This observation corroborates the proposed binding mode by NMR which was further confirmed by isothermal titration calorimetry (ITC) (full details in manuscript III). Lastly, it supports the formation of a symmetric  $[N\cdots C\cdots N]^+$  complex, in which both lobes of the p-orbital of the carbenium ion are involved in an efficient overlap with the nonbonding orbitals of the pyridine nitrogens of the ligand as shown by NMR as otherwise, some conversion would have been observed in the DA reaction.

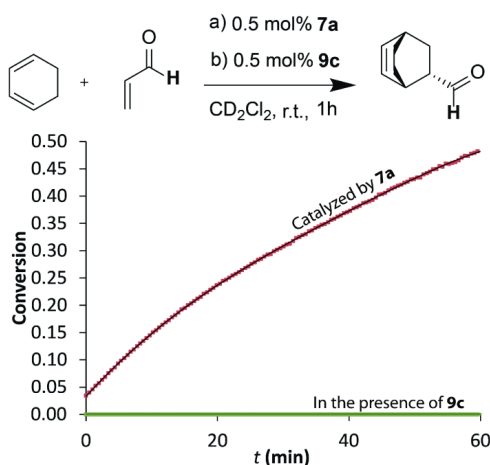


**Figure 20.** The progress of the Diels-Alder condensation, run under literature conditions,<sup>76</sup> of 1,3-cyclohexadiene (1.2 eq) and acrolein (1 mmol) in  $\text{CD}_2\text{Cl}_2$  in the presence of 0.5 mol%

**7a** or **9c** was monitored by  $^1\text{H}$  NMR in an NMR tube at room temperature for 1 hour. The integral of the signals of the aldehyde proton of the starting material and of the product was used to follow the progress of the reaction. Whereas the reaction catalyzed by **7a** (red) progresses with second order rate, the addition of **8c** inhibits it (green) through masking the Lewis acidic **7a** by formation of the strong complex **9c**.

#### 8.4 Summary manuscript III

The first experimental evidence of the synthesis of a stable pentavalent carbonium compound is established by intermolecular interaction. A trivalent carbenium ion is converted into a pentavalent carbonium complex by simultaneous overlap of both lobes of the empty p-orbital of the former species with the nonbonding orbitals of two Lewis bases positioned to form a linear three-center-four-electron  $[\text{N}\cdots\text{C}\cdots\text{N}]^+$  bond. The observation of a single set of NMR between **7** and **8** indicates the formation of a symmetric pentavalent complex whose electron density can be modulated by substitution.  $^{15}\text{N}$  NMR resulted in being a far better measurement tool to  $^{13}\text{C}$  NMR for the detection of formation of the  $[\text{N}\cdots\text{C}\cdots\text{N}]^+$  complex. Similar to the  $\text{S}_{\text{N}}2$  transition state, the central carbon of these complexes form a three-center-four electron bond with a trigonal bi-pyramidal geometry. Therefore, these compounds may be applicable as model systems for the  $\text{S}_{\text{N}}2$  transition state as compared with the previously proposed isoelectronic three-center-four-electron halogen bonds.<sup>77</sup>



## 9. Concluding Remarks

---

This thesis describes the solution investigation of  $[\text{NXN}]^+$  and  $[\text{NCN}]^+$  complexes possessing three center four electron bond. Their stability, symmetry and geometry have been discussed as a whole and the following conclusions were drawn

- In addition to  $^1\text{H}$  NMR, inversion recovery experiments prove the formation and existence of the  $[\text{NCIN}]^+$  complex at low  $-80^\circ\text{C}$ . Geometry optimizations performed at the DFT level suggest that the  $[\text{NCIN}]^+$  complex is symmetric in solution.
- An  $[\text{NFN}]^+$  complex was synthesized, and was demonstrated by NMR and DFT to prefer a static and asymmetric geometry. It is stable at  $-40^\circ\text{C}$  in a  $\text{CD}_3\text{CN}$  solution.
- Using IPE NMR, we have confirmed that  $[\text{NIN}]^+$  complexes are static and symmetric independent of their counterion in both solution and in the solid state, as determined by X-ray diffraction and computation at the DFT level.
- Symmetric  $[\text{NCN}]^+$  complexes are formed upon the interaction of a carbenium with a bidentate nitrogen ligand that provides an optimal orbital overlap with the lobes of the empty p-orbital of the carbenium. In contrast, the carbenium initiates an *N*-alkylation reaction with a monodentate Lewis base. The binding affinity of the carbenium to the bidentate ligand was assessed by calorimetry whereas its structure studied by solution NMR spectroscopy.





## Acknowledgement

---

I would like to take this opportunity to thank all those who have made my experience at the University of Gothenburg a truly wonderful one.

My supervisor Prof. **Máté Erdélyi** –I still remember the day I walked in to your office looking for work. Your enthusiasm and optimism radiated through and I distinctly recall you saying ‘beware - halogen bonding is addictive!’ No words can truly justify the amount of support and constant encouragement I have received from you over the years. Your patience, kindness and your constant availability (night or day) have been truly appreciated. It has been a pleasure working with you and I have so much more to thank you for than space here would allow.

My examiner Prof. **Göran Hilmersson** : thank you for making time for me amidst your extremely busy schedule.

Prof. **Kristina Luthman** : you were so kind to give me feedback on a version of my thesis that was so far from complete. I was feeling incredibly overwhelmed during those days and you always smiled and said ‘it’s all going to be ok.’ I will never forget your warmth and kindness.

Dr. **Hanna Andersson**: I could write an entire page about you! Starting from rides to the airport to constant support and encouragement in the lab, you have been the best mentor anyone could ask for. This experience would have been vastly different without you and every PhD student needs a ‘Hanna’ in their life. I will never forget how much you did for me in the carbocation project when I had to take off. Your patience, kindness and positive energy will always stay with me. I will miss you tremendously.

Dr. **Anna-Carin Carlsson**: Almost everything that I know about the symmetry project today, I know from you. Your knowledge and contribution has been extremely crucial for the design of my projects and your patience while training me during that stressful period before your defense is truly appreciated. It was a lot fun working next to you in the lab and I truly learned a lot from you. All the conferences we attended together and those extra days in Italy will remain cherished memories.

Docent **Jürgen Gräfenstein** and MSc student **Marcus Reitti** for providing wonderful support with the calculations to all the projects. Thank you **Jürgen** for patiently explaining computational details to me and **Marcus** for all the awesome figures. MSc student **Sebastiaan Hakkert** for your editing skills and repeatedly changing the figures till I was content. You came in during your off days to help me out and I truly appreciated the help.

To the best office mate one could ever ask for – Dr. **Mario Janjetovic** you have been missed. Kompis you made me laugh in my worst days and your friendship is invaluable to me. Teaching with you was so much fun - my walking talking google translate!

Dr. **Roland Kleinmaier**, Dr. **Ulrika Brath**, Dr. **Bijan Nekouesihahraki** and Dr. **Patrik Jarvoll** – thank you for all the fun chemistry discussions and tons of NMR. **Ulrika** and **Patrik** – I know I have repeatedly asked the same NMR questions but you were always patient with your answers and I'm truly grateful for that. **Patrik** I will miss that wholehearted laugh of yours! I hope your sense of humor always stays the same. **Bijan** thank you for the tremendous support in the carbocation project. It helped me a lot. Dr. **Inma Lahoz** – your suggestions were always valuable and discussions about chemistry enriching. **Michele Bedin** and the **Rissanen group** – thank you for all the crystal structures for the CI project. The **Sindelar** group for generous amounts of Bambusuril

**Nils Schulz** – thank you for not giving up on ITC and continuing to work on the experiments even after you left GU. I really appreciate the extended effort you made to establish a collaboration with Prof. **Sandro Keller**. Prof. **Sandro** – your input has been so incredibly valuable.

Former labmates **Fatima Ameri**, **Linda Zandi**, **Krenare Mehmeti**, **Manuela Voráčová**, **Eglisa Halluli** and **Måns Andreasson** for always keeping things lively in the group!

Dr. **Emma Danelius** - thank you so much for being my 'Noel' during the writing process. Your constant support and guidance is truly appreciated. **Emma**, **Tina** and **Ivana** – thank you for the 'therapy sessions'. No PhD is truly complete without those. You guys have really been amazing all throughout. **Ivana** – conference trips are the best with you! **Tina** – your kind nature will be truly missed!

**Sweden the gang** – you know who you are. You've been my little family home away from home. You've seen me through my worst and for that, a simple thank you will not suffice. A special shout out to **Oana** and **Gabo** – for a variety of reasons, the thank you list specially for the two of you would truly be endless. **Matt** for re-defining 7<sup>th</sup> of October for me. I love you guys more than you could possibly imagine.

To my **family** – couldn't have made it this far without your constant support. Love you to the moon and back. This ones for you **Bhaiya**.

To my **husband** - the long distance finally ends ☺

This research was funded by The Swedish Research Council and European Research Council.

## References

---

1. Mukherjee, A.; Tothadi, S.; Desiraju, G. R., Halogen bonds in crystal engineering: like hydrogen bonds yet different. *Acc Chem Res* **2014**, *47* (8), 2514-24.
2. Cavallo, G.; Metrangolo, P.; Pilati, T.; Resnati, G.; Sansotera, M.; Terraneo, G., Halogen bonding: a general route in anion recognition and coordination. *Chem Soc Rev* **2010**, *39* (10), 3772-83.
3. Cavallo, G.; Metrangolo, P.; Milani, R.; Pilati, T.; Priimagi, A.; Resnati, G.; Terraneo, G., The Halogen Bond. *Chem Rev* **2016**, *116* (4), 2478-601.
4. Bulfield, D.; Huber, S. M., Halogen Bonding in Organic Synthesis and Organocatalysis. *Chemistry* **2016**, *22* (41), 14434-50.
5. Metrangolo, P.; Resnati, G., Chemistry. Halogen versus hydrogen. *Science* **2008**, *321* (5891), 918-9.
6. Gillis, E. P.; Eastman, K. J.; Hill, M. D.; Donnelly, D. J.; Meanwell, N. A., Applications of Fluorine in Medicinal Chemistry. *Journal of Medicinal Chemistry* **2015**, *58* (21), 8315-8359.
7. Mendez, L.; Henriquez, G.; Sirimulla, S.; Narayan, M., Looking Back, Looking Forward at Halogen Bonding in Drug Discovery. *Molecules* **2017**, *22* (9).
8. Hashizume, D., Experimental Observation of the Nature of Weak Chemical Bonds in Labile Compounds. *Advanced Materials* **2017**, *29* (25).
9. Yamamoto, Y.; Akiba, K. Y., Synthesis of hypervalent pentavalent carbon and boron compounds. *J Syn Org Chem Jpn* **2004**, *62* (11), 1128-1137.
10. Fernandez, I.; Uggerud, E.; Frenking, G., Stable pentacoordinate carbocations: Structure and bonding. *Chem-Eur J* **2007**, *13* (30), 8620-8626.
11. Cavallo, G.; Metrangolo, P.; Pilati, T.; Resnati, G.; Terraneo, G., Halogen bond: a long overlooked interaction. *Top Curr Chem* **2015**, *358*, 1-17.
12. Desiraju, G. R.; Ho, P. S.; Kloo, L.; Legon, A. C.; Marquardt, R.; Metrangolo, P.; Politzer, P.; Resnati, G.; Rissanen, K., Definition of the halogen bond (IUPAC Recommendations 2013). *Pure Appl Chem* **2013**, *85* (8), 1711-1713.
13. Hassel, O.; Hvoslef, J., The Structure of Bromine 1,4-Dioxanate. *Acta Chem Scand* **1954**, *8* (5), 873-873.
14. Dumas, J. M.; Peurichard, H.; Gomel, M., Cx4...Base Interactions as Models of Weak Charge-Transfer Interactions - Comparison with Strong Charge-Transfer and Hydrogen-Bond Interactions. *J Chem Res-S* **1978**, (2), 54-55.
15. Farina, A.; Meille, S. V.; Messina, M. T.; Metrangolo, P.; Resnati, G.; Vecchio, G., Resolution of racemic 1,2-dibromohexafluoropropane through halogen-bonded supramolecular helices. *Angew Chem Int Edit* **1999**, *38* (16), 2433-2436.
16. (a) Clark, T.; Hennemann, M.; Murray, J. S.; Politzer, P., Halogen bonding: the sigma-hole. *J Mol Model* **2007**, *13* (2), 291-296; (b) Cavallo, G.; Murray, J. S.; Politzer, P.; Pilati, T.; Ursini, M.; Resnati, G., Halogen bonding in hypervalent iodine and bromine derivatives: halonium salts. *Iucrj* **2017**, *4*, 411-419.
17. (a) Politzer, P.; Murray, J. S.; Clark, T., Halogen bonding and other sigma-hole interactions: a perspective. *Physical Chemistry Chemical Physics* **2013**, *15* (27), 11178-11189; (b) Politzer, P.; Murray, J. S.; Clark, T., Halogen bonding: an electrostatically-driven highly directional noncovalent interaction. *Physical Chemistry Chemical Physics* **2010**, *12* (28), 7748-7757.
18. Wang, C.; Danovich, D.; Mo, Y.; Shaik, S., On The Nature of the Halogen Bond. *J Chem Theory Comput* **2014**, *10* (9), 3726-37.

19. Carlsson, A. C. C.; Veiga, A. X.; Erdelyi, M., Halogen Bonding in Solution. *Top Curr Chem* **2015**, *359*, 49-76.
20. Metrangolo, P.; Neukirch, H.; Pilati, T.; Resnati, G., Halogen bonding based recognition processes: a world parallel to hydrogen bonding. *Acc Chem Res* **2005**, *38* (5), 386-95.
21. (a) Bertran, J. F.; Rodriguez, M., Detection of Halogen Bond Formation by Correlation of Proton Solvent Shifts .2. Methylene Halides in N-Electron Donor Solvents. *Org Magn Resonance* **1980**, *14* (4), 244-246; (b) Bertran, J. F.; Rodriguez, M., Detection of Halogen Bond Formation by Correlation of Proton Solvent Shifts .1. Haloforms in Normal-Electron Donor Solvents. *Org Magn Resonance* **1979**, *12* (2), 92-94.
22. Rissanen, K.; Haukka, M., Halonium Ions as Halogen Bond Donors in the Solid State [XL2]Y Complexes. *Top Curr Chem* **2015**, *359*, 77-90.
23. Corradi, E.; Meille, S. V.; Messina, M. T.; Metrangolo, P.; Resnati, G., Perfluorocarbon-hydrocarbon self-assembly, part IX. Halogen bonding versus hydrogen bonding in driving self-assembly processes. *Angew Chem Int Edit* **2000**, *39* (10), 1782.
24. Bulfield, D.; Huber, S. M., Halogen Bonding in Organic Synthesis and Organocatalysis. *Chem-Eur J* **2016**, *22* (41), 14434-14450.
25. Rowe, R. K.; Ho, P. S., Relationships between hydrogen bonds and halogen bonds in biological systems. *Acta Crystallogr B* **2017**, *73*, 255-264.
26. Shields, Z. P.; Murray, J. S.; Politzer, P., Directional Tendencies of Halogen and Hydrogen Bonds. *Int J Quantum Chem* **2010**, *110* (15), 2823-2832.
27. (a) Desiraju, G. R., A Bond by Any Other Name. *Angew Chem Int Edit* **2011**, *50* (1), 52-59; (b) Aakeroy, C. B.; Panikkattu, S.; Chopade, P. D.; Desper, J., Competing hydrogen-bond and halogen-bond donors in crystal engineering. *Crystengcomm* **2013**, *15* (16), 3125-3136.
28. Corradi, E.; Meille, S. V.; Messina, M. T.; Metrangolo, P.; Resnati, G., Halogen Bonding versus Hydrogen Bonding in Driving Self-Assembly Processes Perfluorocarbon-hydrocarbon self-assembly, part IX. This work was supported by MURST (Cofinanziamento '99) and EU (COST-D12-0012). We thank Dr. A. Lunghi and Dr. P. Cardillo (Stazione Sperimentale Combustibili, S. Donato Milanese, Italy) for ARC experiments. Part VIII: ref. 9. *Angew Chem Int Ed Engl* **2000**, *39* (10), 1782-1786.
29. Baldrighi, M.; Cavallo, G.; Chierotti, M. R.; Gobetto, R.; Metrangolo, P.; Pilati, T.; Resnati, G.; Terraneo, G., Halogen bonding and pharmaceutical cocrystals: the case of a widely used preservative. *Mol Pharm* **2013**, *10* (5), 1760-72.
30. Amico, V.; Meille, S. V.; Corradi, E.; Messina, M. T.; Resnati, G., Perfluorocarbon-hydrocarbon self-assembly. 1D infinite chain formation driven by nitrogen center dot center dot center dot iodine interactions. *J Am Chem Soc* **1998**, *120* (32), 8261-8262.
31. Turunen, L.; Peuronen, A.; Forsblom, S.; Kalenius, E.; Lahtinen, M.; Rissanen, K., Tetrameric and Dimeric [NI<sup>+</sup> N] Halogen-Bonded Supramolecular Cages. *Chemistry* **2017**, *23* (48), 11714-11718.
32. Beyeh, N. K.; Pan, F.; Rissanen, K., A Halogen-Bonded Dimeric Resorcinarene Capsule. *Angew Chem Int Ed Engl* **2015**, *54* (25), 7303-7.
33. Turunen, L.; Warzok, U.; Puttreddy, R.; Beyeh, N. K.; Schalley, C. A.; Rissanen, K., [NI<sup>+</sup> N] Halogen-Bonded Dimeric Capsules from Tetrakis(3-pyridyl)ethylene Cavitands. *Angew Chem Int Ed Engl* **2016**, *55* (45), 14033-14036.
34. Walter, S. M.; Kniep, F.; Herdtweck, E.; Huber, S. M., Halogen-bond-induced activation of a carbon-heteroatom bond. *Angew Chem Int Ed Engl* **2011**, *50* (31), 7187-91.
35. Cavallo, G.; Murray, J. S.; Politzer, P.; Pilati, T.; Ursini, M.; Resnati, G., Halogen bonding in hypervalent iodine and bromine derivatives: halonium salts. *IUCrJ* **2017**, *4* (Pt 4), 411-419.
36. Olah, G. A., My Search for Carbocations and Their Role in Chemistry (Nobel Lecture). *Angewandte Chemie-International Edition in English* **1995**, *34* (13-14), 1393-1405.

37. Olah, G. A., 100 years of carbocations and their significance in chemistry. *J Org Chem* **2001**, *66* (18), 5943-57.
38. Akiba, K. Y.; Moriyama, Y.; Mizozoe, M.; Inohara, H.; Nishii, T.; Yamamoto, Y.; Minoura, M.; Hashizume, D.; Iwasaki, F.; Takagi, N.; Ishimura, K.; Nagase, S., Synthesis and characterization of stable hypervalent carbon compounds (10-C-5) bearing a 2,6-bis(p-substituted phenyloxymethyl)benzene ligand. *J Am Chem Soc* **2005**, *127* (16), 5893-5901.
- 39.(a) Yamashita, M.; Yamamoto, Y.; Akiba, K. Y.; Hashizume, D.; Iwasaki, F.; Takagi, N.; Nagase, S., Syntheses and structures of hypervalent pentacoordinate carbon and boron compounds bearing an anthracene skeleton - Elucidation of hypervalent interaction based on X-ray analysis and DFT calculation. *J Am Chem Soc* **2005**, *127* (12), 4354-4371; (b) Akiba, K.; Yamashita, M.; Yamamoto, Y.; Nagase, S., Synthesis and isolation of stable hypervalent carbon compound (10-C-5) bearing a 1,8-dimethoxyanthracene ligand. *J Am Chem Soc* **1999**, *121* (45), 10644-10645.
- 40.(a) Carlsson, A. C. C.; Mehmeti, K.; Uhrbom, M.; Karim, A.; Bedin, M.; Puttreddy, R.; Kleinmaier, R.; Neverov, A. A.; Nekoueishahraki, B.; Grafenstein, J.; Rissanen, K.; Erdelyi, M., Substituent Effects on the [N-I-N](+) Halogen Bond. *J Am Chem Soc* **2016**, *138* (31), 9853-9863; (b) Carlsson, A. C. C.; Uhrbom, M.; Karim, A.; Brath, U.; Grafenstein, J.; Erdelyi, M., Solvent effects on halogen bond symmetry. *Crystengcomm* **2013**, *15* (16), 3087-3092; (c) Carlsson, A. C. C.; Grafenstein, J.; Budnjo, A.; Laurila, J. L.; Bergquist, J.; Karim, A.; Kleinmaier, R.; Brath, U.; Erdelyi, M., Symmetric Halogen Bonding Is Preferred in Solution. *J Am Chem Soc* **2012**, *134* (12), 5706-5715; (d) Carlsson, A. C. C.; Grafenstein, J.; Laurila, J. L.; Bergquist, J.; Erdelyi, M., Symmetry of [N-X-N](+) halogen bonds in solution. *Chem Commun* **2012**, *48* (10), 1458-1460.
41. Snyder, S. A.; Treitler, D. S.; Brucks, A. P., Simple Reagents for Direct Halonium-Induced Polyene Cyclizations. *J Am Chem Soc* **2010**, *132* (40), 14303-14314.
42. Okitsu, T.; Yumitate, S.; Sato, K.; In, Y.; Wada, A., Substituent Effect of Bis(pyridines)iodonium Complexes as Iodinating Reagents: Control of the Iodocyclization/Oxidation Process. *Chem-Eur J* **2013**, *19* (16), 4992-4996.
- 43.(a) Barluenga, J., Transferring iodine: more than a simple functional group exchange in organic synthesis. *Pure Appl Chem* **1999**, *71* (3), 431-436; (b) Barluenga, J.; Rodriguez, M. A.; Campos, P. J., Electrophilic Additions of Positive Iodine to Alkynes through an Iodonium Mechanism. *J Org Chem* **1990**, *55* (10), 3104-3106.
- 44.(a) Gonzalez, J. M.; Muniz, K., Jose Barluenga (1940-2016) Obituary. *Angew Chem Int Edit* **2016**, *55* (49), 15208-15208; (b) Murai, K.; Tateishi, K.; Saito, A., Barluenga's reagent with HBF<sub>4</sub> as an efficient catalyst for alkyne-carbonyl metathesis of unactivated alkynes. *Organic & Biomolecular Chemistry* **2016**, *14* (44), 10352-10356.
45. Blair, L. K.; Parris, K. D.; Hii, P. S.; Brock, C. P., A Stable Br<sup>+</sup> Complex - a Twisted Bicyclo[2.2.2]Octane Derivative - Synthesis and Structure of Bis(Quinuclidine)Bromine(I) Tetrafluoroborate. *J Am Chem Soc* **1983**, *105* (11), 3649-3653.
46. Haque, I.; Wood, J. L., Vibrational Spectra and Structure of Bis(Pyridine)Iodine(I) Bis(Pyridine)Bromine(I) Bis(Gamma-Picoline)Iodine(I) and Bis(Gamma-Picoline)Bromine(I) Cations. *J Mol Struct* **1968**, *2* (3), 217.
47. Hakkert, S. B.; Grafenstein, J.; Erdelyi, M., The 15N NMR chemical shift in the characterization of weak halogen bonding in solution. *Faraday Discuss* **2017**.
48. Kong, S.; Borissova, A. O.; Lesnichin, S. B.; Hartl, M.; Daemen, L. L.; Eckert, J.; Antipin, M. Y.; Shenderovich, I. G., Geometry and spectral properties of the protonated homodimer of pyridine in the liquid and solid states. A combined NMR, X-ray diffraction and inelastic neutron scattering study. *J Phys Chem A* **2011**, *115* (27), 8041-8.

- 49.(a) Perrin, C. L.; Ohta, B. K., Symmetry of NHN hydrogen bonds in solution. *J Mol Struct* **2003**, *644* (1-3), 1-12; (b) Perrin, C. L.; Ohta, B. K., Symmetry of O-H-O and N-H-N hydrogen bonds in 6-hydroxy-2-formylfulvene and 6-aminofulvene-2-aldehydes. *Bioorganic Chemistry* **2002**, *30* (1), 3-15; (c) Perrin, C. L.; Ohta, B. K., Symmetry of N-H-N hydrogen bonds in 1,8-Bis(dimethylamino)naphthalene center dot H<sup>+</sup> and 2,7-dimethoxy-1,8-bis(dimethylamino)naphthalene center dot H<sup>+</sup>. *J Am Chem Soc* **2001**, *123* (27), 6520-6526; (d) Perrin, C. L.; Ohta, B. K., Symmetry of NHN hydrogen bonds in solution. *Abstr Pap Am Chem S* **2001**, *221*, U211-U211; (e) Perrin, C. L.; Nielson, J. B., Symmetries of hydrogen bonds in solution. *Abstr Pap Am Chem S* **1997**, *213*, 249-Orgn.
- 50.Georgiou, D. C.; Butler, P.; Browne, E. C.; Wilson, D. J. D.; Dutton, J. L., On the Bonding in Bis-pyridine Iodonium Cations. *Aust J Chem* **2013**, *66* (10), 1179-1188.
- 51.Emsley, J., Very Strong Hydrogen-Bonding. *Chem Soc Rev* **1980**, *9* (1), 91-124.
- 52.Bartoszak, E.; Jaskolski, M.; Grech, E.; Gustafsson, T.; Olovsson, I., Structure of Thiocyanate Salt of 1,8-Bis(Dimethylamino)Naphthalene (Dmanh<sup>+</sup>.Scn<sup>-</sup>) at 188 and 290 K. *Acta Crystallographica Section B-Structural Science* **1994**, *50*, 358-363.
- 53.(a) Glowiak, T.; Majerz, I.; Malarski, Z.; Sobczyk, L.; Pozharskii, A. F.; Ozeryanskii, V. A.; Grech, E., Structure and IR spectroscopic behaviour of 2,7-dichloro-1,8-bis(dimethylamino)naphthalene and its protonated form. *J Phys Org Chem* **1999**, *12* (12), 895-900; (b) Grech, E.; Malarski, Z.; Sawka-Dobrowolska, W.; Sobczyk, L., Low-temperature (120 K) structure and vibrational spectrum of protonated proton sponge: the adduct of 1,8-bis(dimethylamino)naphthalene (DMAN) with 4,5-dicyanoimidazole (DCI). *J Phys Org Chem* **1999**, *12* (4), 313-318.
- 54.Kleinberg, J., Reactions of the Halogens with the Silver Salts of Carboxylic Acids. *Chemical Reviews* **1947**, *40* (3), 381-390.
- 55.(a) Zingaro, R. A.; Vanderwerf, C. A.; Kleinberg, J., Evidence for the Existence of Unipositive Iodine Ion in Solutions of Iodine in Pyridine. *J Am Chem Soc* **1951**, *73* (1), 88-90; (b) Zingaro, R. A.; Witmer, W. B.; Kauffman, G. B.; Stevens, K. L., Unipositive Halogen Complexes. *Inorg Syn* **1963**, *7*, 169-176.
- 56.(a) Zingaro, R. A.; Vanderwerf, C. A.; Kleinberg, J., Further Observations on the Preparation and Reactions of Positive Iodine Salts. *J Am Chem Soc* **1950**, *72* (11), 5341-5342; (b) Zingaro, R. A.; Goodrich, J. E.; Kleinberg, J.; Vanderwerf, C. A., Reactions of the Silver Salts of Carboxylic Acids with Iodine in the Presence of Some Tertiary Amines. *J Am Chem Soc* **1949**, *71* (2), 575-576; (c) Rubenacker, G. V.; Brown, T. L., N-14 Nuclear-Quadrupole Resonance-Spectra of Coordinated Pyridine - Extended Evaluation of the Coordinated Nitrogen Model. *Inorg Chem* **1980**, *19* (2), 392-398.
- 57.(a) Carlsson, A. C.; Mehmeti, K.; Uhrbom, M.; Karim, A.; Bedin, M.; Puttreddy, R.; Kleinmaier, R.; Neverov, A. A.; Nekoueishahraki, B.; Grafenstein, J.; Rissanen, K.; Erdelyi, M., Substituent Effects on the [N-I-N](+) Halogen Bond. *J Am Chem Soc* **2016**, *138* (31), 9853-63; (b) Carlsson, A. C.; Grafenstein, J.; Budnjo, A.; Laurila, J. L.; Bergquist, J.; Karim, A.; Kleinmaier, R.; Brath, U.; Erdelyi, M., Symmetric halogen bonding is preferred in solution. *J Am Chem Soc* **2012**, *134* (12), 5706-15; (c) Carlsson, A. C.; Grafenstein, J.; Laurila, J. L.; Bergquist, J.; Erdelyi, M., Symmetry of [N-X-N]<sup>+</sup> halogen bonds in solution. *Chem Commun (Camb)* **2012**, *48* (10), 1458-60.
- 58.Perrin, C. L., Symmetry of hydrogen bonds in solution. *Pure Appl Chem* **2009**, *81* (4), 571-583.
- 59.Hansen, P. E., Isotope effects on chemical shifts in the study of intramolecular hydrogen bonds. *Molecules* **2015**, *20* (2), 2405-24.
- 60.(a) Saunders, M.; Telkowski, L.; Kates, M. R., Isotopic Perturbation of Degeneracy - C-13 Nuclear Magnetic-Resonance Spectra of Dimethylcyclopentyl and Dimethylnorbonyl Cations. *J Am Chem Soc* **1977**, *99* (24), 8070-8071; (b) Perrin, C. L.; Burke, K. D., Variable-

Temperature Study of Hydrogen-Bond Symmetry in Cyclohexene-1,2-dicarboxylate Monoanion in Chloroform-d. *J Am Chem Soc* **2014**, *136* (11), 4355-4362; (c) Perrin, C. L.; Karri, P.; Moore, C.; Rheingold, A. L., Hydrogen-Bond Symmetry in Difluoromaleate Monoanion. *J Am Chem Soc* **2012**, *134* (18), 7766-7772.

61. Perrin, C. L.; Flach, A., No contribution of an inductive effect to secondary deuterium isotope effects on acidity. *Angew Chem Int Ed Engl* **2011**, *50* (33), 7674-6.

62. Weston, R. E., The Magnitude of Electronic Isotope Effects. *Tetrahedron* **1959**, *6* (1), 31-35.

63. Perrin, C. L., Are Short, Low-Barrier Hydrogen Bonds Unusually Strong? *Accounts Chem Res* **2010**, *43* (12), 1550-1557.

64. Perrin, C. L.; Dong, Y. M., Secondary deuterium isotope effects on the acidity of carboxylic acids and phenols. *J Am Chem Soc* **2007**, *129* (14), 4490-4497.

65. van't Hoff, J. H. Z., *Z. Phys. Chem.* **1887**, *1*, 783.

66. Strauss, C. R.; Trainor, R. W., Invited Review - Developments in Microwave-Assisted Organic-Chemistry. *Aust J Chem* **1995**, *48* (10), 1665-1692.

67. Kong, S.; Borissova, A. O.; Lesnichin, S. B.; Hartl, M.; Daemen, L. L.; Eckert, J.; Antipin, M. Y.; Shenderovich, I. G., Geometry and Spectral Properties of the Protonated Homodimer of Pyridine in the Liquid and Solid States. A Combined NMR, X-ray Diffraction and Inelastic Neutron Scattering Study. *J Phys Chem A* **2011**, *115* (27), 8041-8048.

68. (a) Carlsson, A.-C. C.; Graefenstein, J.; Budnjo, A.; Laurila, J. L.; Bergquist, J.; Karim, A.; Kleinmaier, R.; Brath, U.; Erdelyi, M., Symmetric Halogen Bonding Is Preferred in Solution. *Journal of the American Chemical Society* **2012**, *134* (12), 5706-5715; (b) Carlsson, A.-C. C.; Graefenstein, J.; Laurila, J. L.; Bergquist, J.; Erdelyi, M., Symmetry of [N-X-N]<sup>+</sup> halogen bonds in solution. *Chemical Communications (Cambridge, United Kingdom)* **2012**, *48* (10), 1458-1460; (c) Hakkert, S. B.; Erdelyi, M., Halogen bond symmetry: the N-X-N bond. *J. Phys. Org. Chem.* **2015**, *28*, 226-233;

69. (a) Havel, V.; Svec, J.; Wimmerova, M.; Dusek, M.; Pojarova, M.; Sindelar, V., Bambus[n]urils: a new family of macrocyclic anion receptors. *Organic Letters* **2011**, *13* (15), 4000-4003; (b) Svec, J.; Necas, M.; Sindelar, V., Bambus[6]uril. *Angew Chem Int Edit* **2010**, *49* (13), 2378-81.

70. Rissanen, K.; Haukka, M., Halonium Ions as Halogen Bond Donors in the Solid State [XL2]Y Complexes. *Top Curr Chem* **2015**, *359*, 77-90.

71 (b) Hakkert, S. B.; Grafenstein, J.; Erdelyi, M., The 15N NMR chemical shift in the characterization of weak halogen bonding in solution. *Faraday Discuss.* **2017**; (c) Carlsson, A.-C. C.; Grafenstein, J.; Budnjo, A.; Laurila, J. L.; Bergquist, J.; Karim, A.; Kleinmaier, R.; Brath, U.; Erdelyi, M., Symmetric halogen bonding is preferred in solution. *J. Am. Chem. Soc.* **2012**, *134* (12), 5706.

72. Carlsson, A.-C. C.; Mehmeti, K.; Uhrbom, M.; Karim, A.; Bedin, M.; Puttreddy, R.; Kleinmaier, R.; Neverov, A. A.; Nekoueishahraki, B.; Grafenstein, J.; Rissanen, K.; Erdelyi, M., Substituent Effects on the [N-I-N]<sup>(+)</sup> Halogen Bond. *J. Am. Chem. Soc.* **2016**, *138* (31), 9853-9863.

73. Bah, J.; Naidu, V. R.; Teske, J.; Franzen, J., Carbocations as Lewis Acid Catalysts: Reactivity and Scope. *Adv Synth Catal* **2015**, *357* (1), 148-158.

74. (a) Andersson, H.; Carlsson, A.-C. C.; Nekoueishahraki, B.; Brath, U.; Erdelyi, M., Solvent Effects on Nitrogen Chemical Shifts. *Annu. Rep. NMR Spectrosc.* **2015**, *86*, 73-210; (b) Hakkert, S. B.; Erdelyi, M., Halogen bond symmetry: the N-X-N bond. *J. Phys. Org. Chem.* **2015**, *28* (3), 226-233.

75. Carlsson, A.-C. C.; Mehmeti, K.; Uhrbom, M.; Karim, A.; Bedin, M.; Puttreddy, R.; Kleinmaier, R.; Neverov, A. A.; Nekoueishahraki, B.; Grafenstein, J.; Rissanen, K.; Erdelyi,

M., Substituent Effects on the [N-I-N](+) Halogen Bond. *J. Am. Chem. Soc.* **2016**, *138* (31), 9853-9863.

76. Bah, J.; Franzen, J., Carbocations as Lewis acid catalysts in Diels-Alder and Michael addition reactions. *Chem. Eur. J.* **2014**, *20* (4), 1066-72.

77.(a) Firestone, R. A., Application of Linnett Electronic Theory to Organic Chemistry .4. Sn2 Transition State. *J. Org. Chem.* **1971**, *36* (5), 702;